SAPIENZA
UNIVERSITÀ DI ROMA

Department of Mechanical and Aerospace Engineering

SSD ING-IND/14 Machine Design group

Research activities

People:

Giovanni Broggiato (PA)

Luca Cortese (RTD-B)

Filippo Nalli (PhD)

February 8, 2017

Outline of main research activities

SAPIENZA UNIVERSITÀ DI ROMA

Experimental Mechanics related activities and FE analysis

- Multiaxial tests for assessment of materials structural performance
- Ad hoc tests on components or mechanical systems.
- Devising of custom-made equipment, for non conventional tests execution
- Finite Element modelling of structural and thermo-structural problems

Modelling of elasto-plastic material behaviour, ductile damage accumulation and fracture prediction

- Calibration methodology for numerical models
- Devising of original plasticity and damage models
- Experimental characterization, focus on bulk materials, additive manufacturing, and sheet metals

Measurement techniques with Digital Image Correlation

Experimental-numerical techniques for the restoration of Cultural Heritage

Ongoing research activities

Experimental Mechanics activities and FE Analysis

- Investigated materials
- Testing using standard equipment
- Tension-torsion biaxial machine and multiaxial tests
- Finite Elements as a complementary tool in testing

Materials

Investigated so far, some of them presented here:

- Different steel grades for pipeline (oil and gas) or general (automotive) applications: ***Grade X52, Grade X65, Grade X100, 33MnB5.***
- High strength steels used for sheets: ***HSLA, DP, TriP, TwiP.***
- **Titanium *Ti6Al4V* alloy**

Experimental activities, FEA
Universal testing machine

SAPIENZA
UNIVERSITÀ DI ROMA

- Equipment: servo-hydraulic MTS machine, for static, fatigue and cyclic testing

- Specifications:

  - *250 kN* maximum load
  - *150 mm* stroke
  - Sensors: load cell, lvdt transducer and estensometer
  - Grips: threads for round specimens, wedges for flat specimens, plates for compressions, punch and die for three-point bend.
  - Acquisition system: NI card and Labview software

- Equipment: Custom-made electro-mechanical biaxial machine

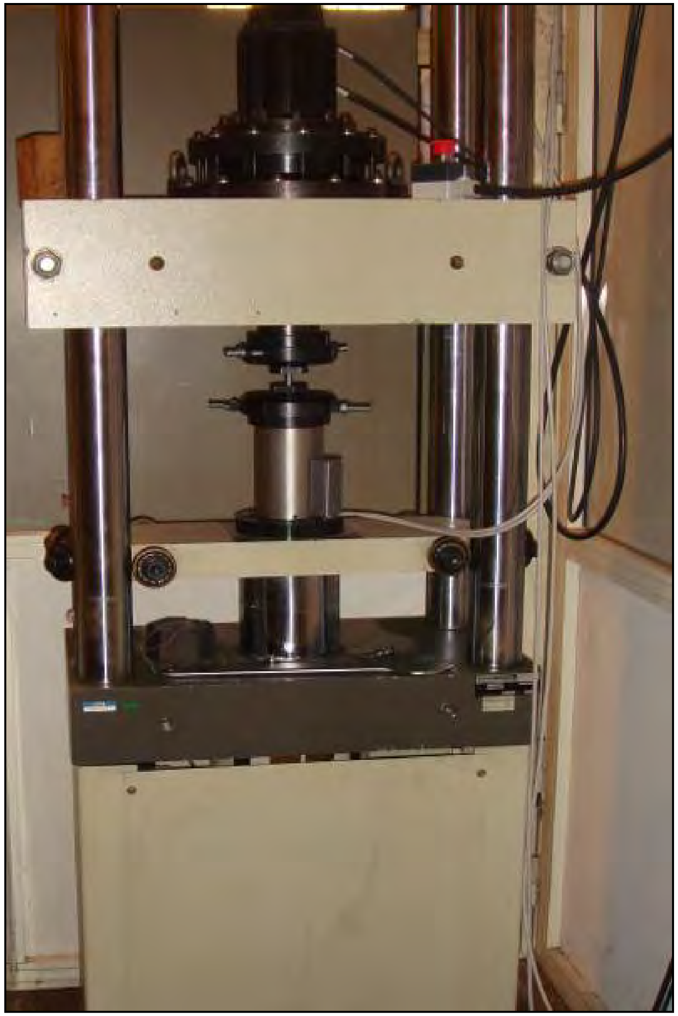

- Specifications:

- *100kN* maximum axial load
- *150 mm* axial stroke
- *1000 Nm* maximum torsional load
- Unlimited rotation angle
- Sensors: biaxial load cell, linear and rotational displacement acquision by digital encoders
- Control and acquisition system: NI FPGA card and Labview software.

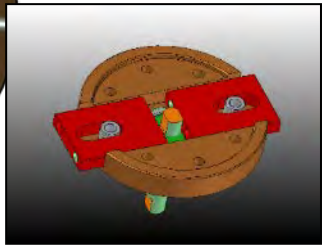

Experimental activities, FEA

Test details

- Experiments: tensile, round notched, compression and torsion tests

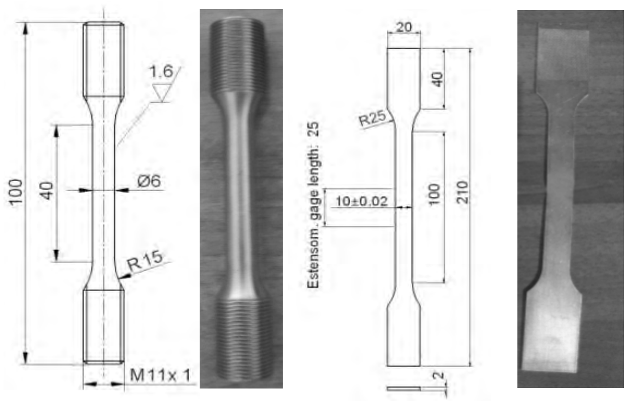

Geometry configuration of specimens: flat and smooth cylindrical bars for uniaxial tensile test.

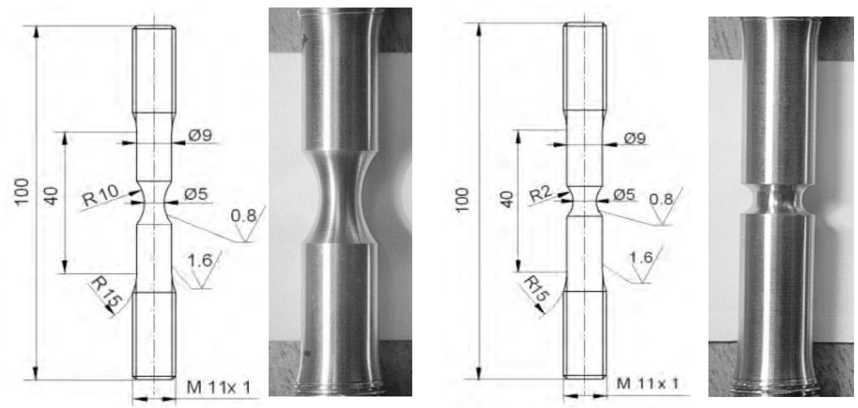

Geometry configuration of specimens: round notched bars (notch radius 2 and 10 mm) for triaxial tensile test.

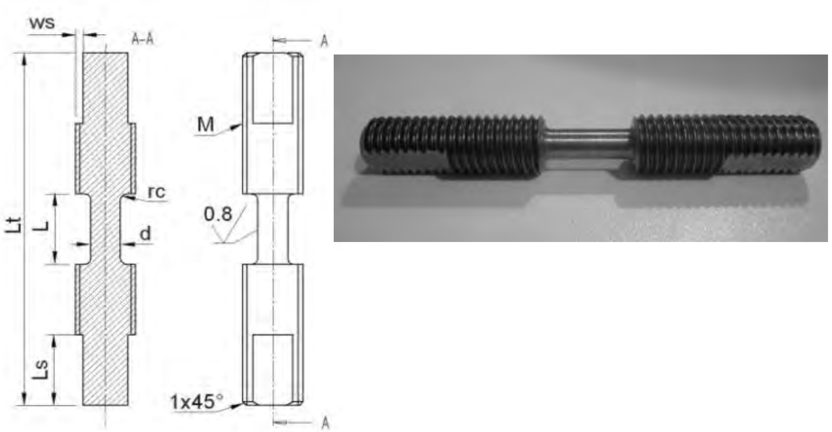

Geometry configuration of specimens: cylindrical bars for torsion test.

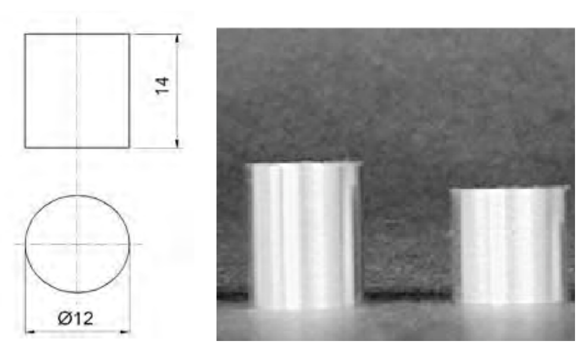

Geometry configuration of specimens: barreled cylinders for compression test.

- Experiments: plain strain and three-point bend

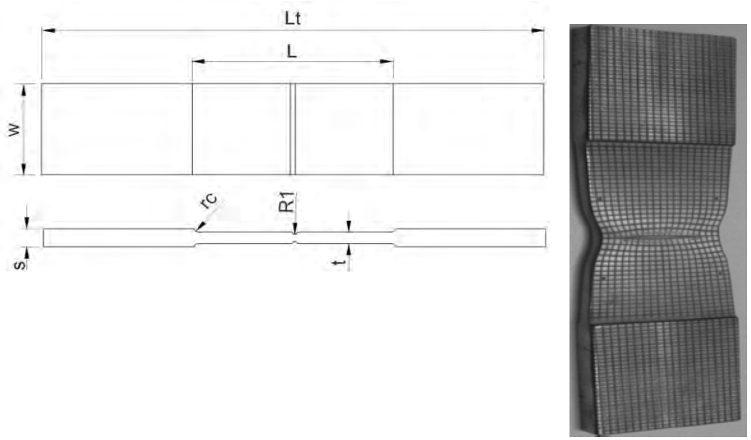

Geometry configuration of specimens: grooved large strips for plane strain tensile test.

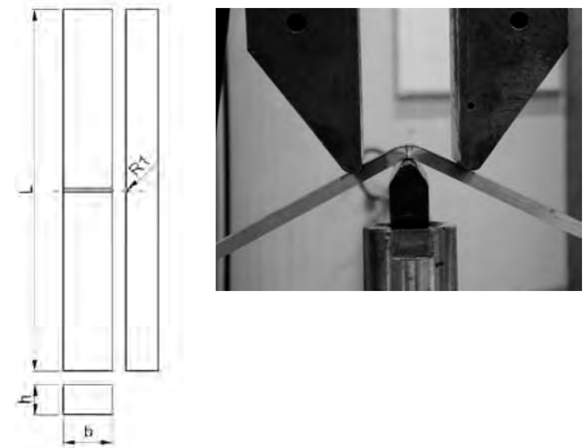

Geometry configuration of specimens: grooved strips for three-point bend test.

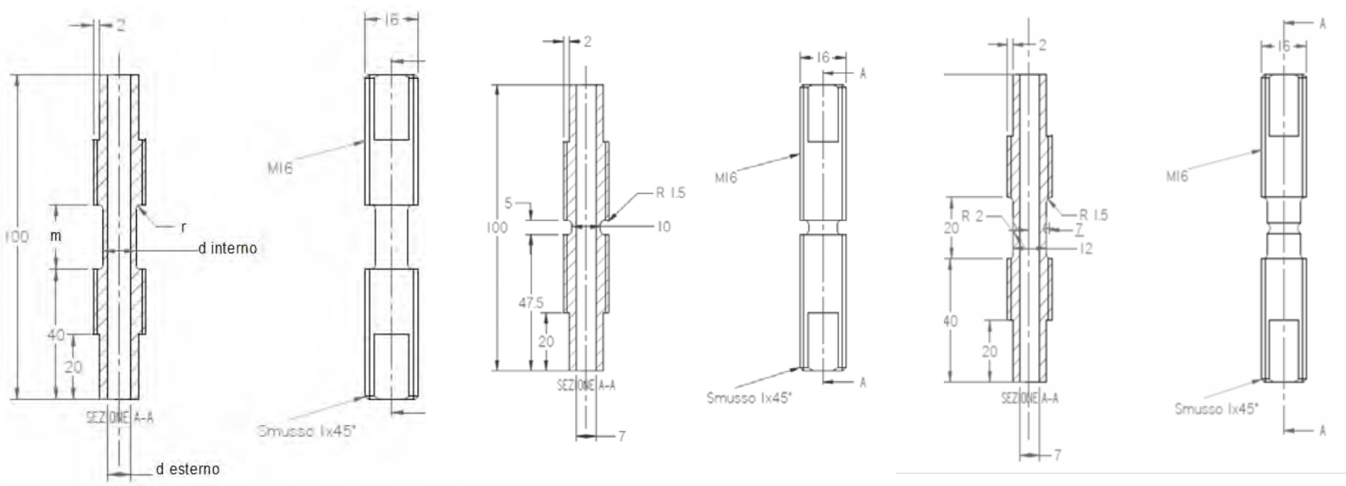

Experimental activities, FEA

2D Axisymmetric and 3D FE Models

- Indirect measurements from FE analysis: local quantities at critical points (stress paths, strain to failure ε_f, ….).

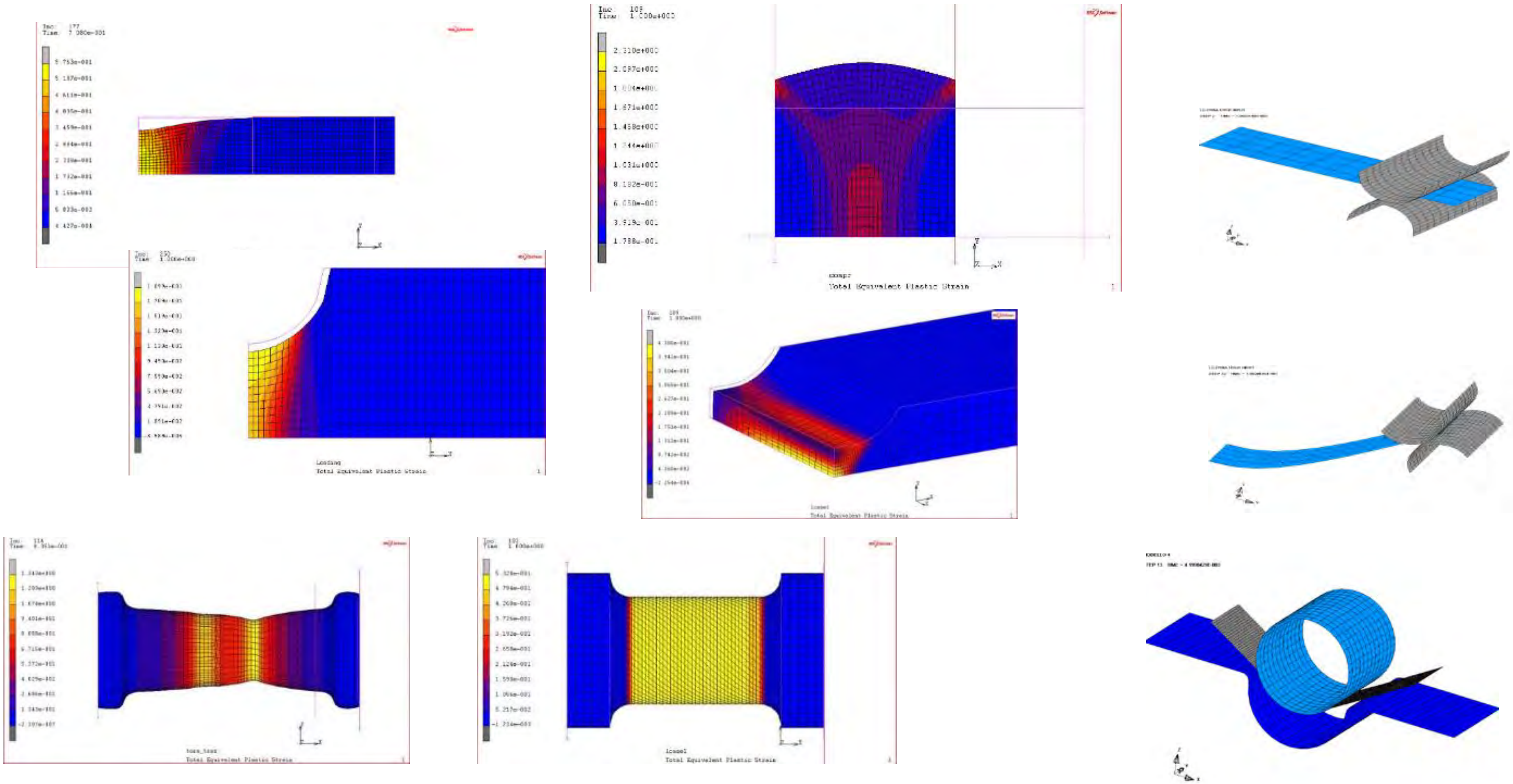

Numerical simulations with MSC Marc, Ansys and LS-Dyna FE codes

Numerical models:
plasticity and ductile damage prediction

- Isotropic J2 plasticity
- Inverse methods for identification of plasticity model parameters
- Torsion as an alternative to tension test
- Isotropic-kinematic combined models for cyclic plasticity
- J2-J3 isotropic plasticity model
- Linear Damage models based on triaxiality and deviatoric parameters
- Nonlinear damage models
- Prospective application fields

- Material characterization at large strain: **inverse methods identification.** matching of experimental and corresponding FE data by means of an optimization algorithm.

Necking strain

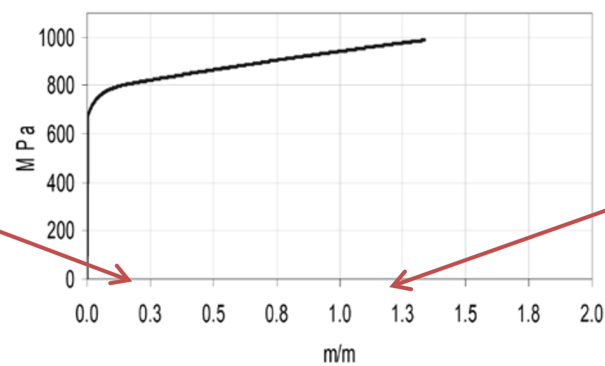

Failure strain

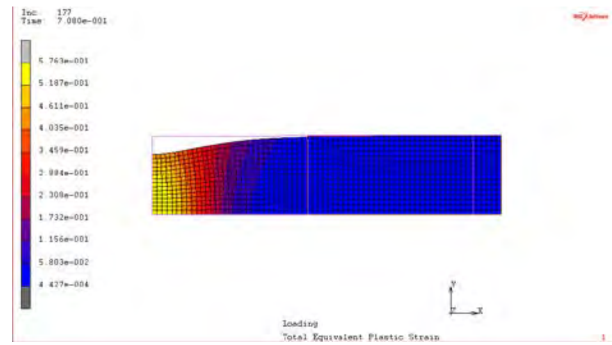

Fe simulation of tensile tests

Stress-strain curve: no significant data available after necking from a tensile test (occurring at few % of plastic strain). Ductile materials fail at a much higher plastic deformation.

Linear weighted (*w*) combination of a tangent and power law post-necking extrapolation:

$$\sigma = \sigma_u \left[w\left(1+\varepsilon-\varepsilon_u\right)+\left(1-w\right)\left(\frac{\varepsilon^{\varepsilon_u}}{\varepsilon_u^{\ \varepsilon_u}}\right)\right]$$

Other analytical expressions (usually take 2 or more parameters):

$$\sigma = K(\varepsilon_0+\varepsilon_p)^n$$

$$\sigma = \sigma_0 + A(1-e^{-b\varepsilon_p})$$

- Large strain stress-strain fit results.

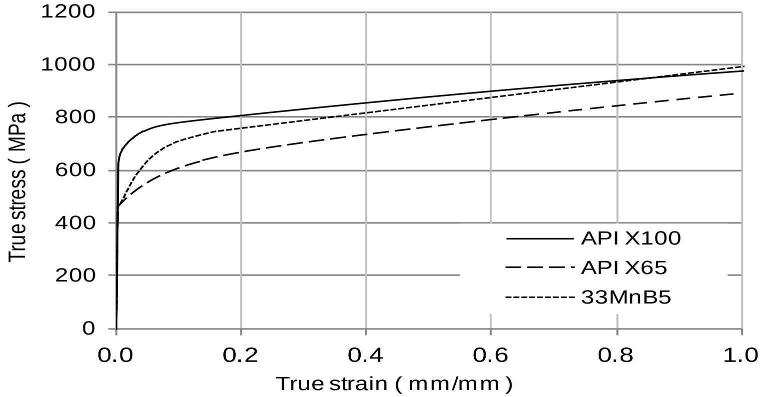

Grade X100, Grade X65, 33MnB5 Extended stress-strain curves, from tensile tests

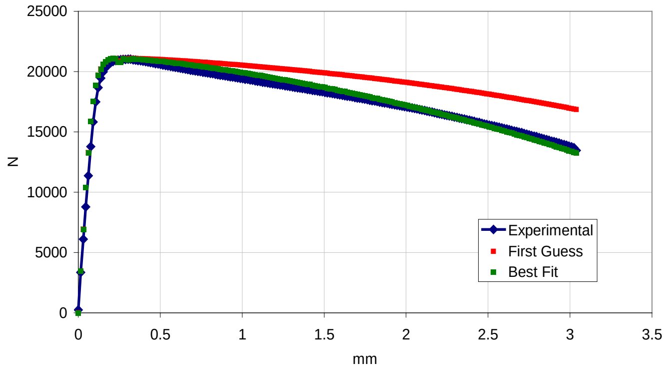

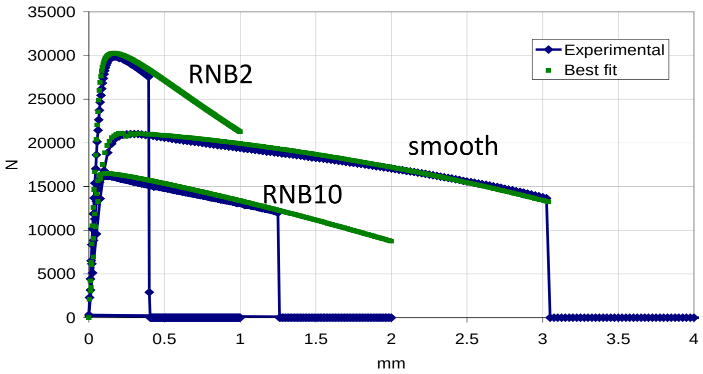

Calibration and validation at laboratory level on different (notched) specimen geometries. Material: 33MnB5

- ***G.B. Broggiato, L. Cortese, (2009) White-light speckle image correlation applied to large-strain material characterization, European Journal of Computational Mechanics, Volume 18-No.3-4/2009. p. 377-392.***

Numerical models: plasticity

Torsion as an alternative to tension test

SAPIENZA UNIVERSITÀ DI ROMA

- Torsion test: the material stress-strain curve can be identified experimentally up to very large strain (no necking occurrence).

Experimental data post-processing: direct fit of experimental M-θ data

$$M = \int_0^{r_0} 2\pi r^2 \tau(\gamma) dr$$

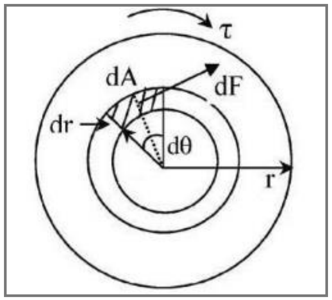

Analytical expressions for the constitutive behaviour:

$$\tau = G\gamma \qquad \gamma = r\frac{d\vartheta}{dz}$$

$$\tau = \tau_s + k(\gamma - \gamma_s)^n$$

$$\tau = \tau_s + A\left(1 - e^{-B(\gamma-\gamma_s)}\right) + C(\gamma - \gamma_s)$$

Alternative: The Nadai's approach:

$$\tau(\gamma_0) = \frac{1}{2\pi r_0^3}\left(\vartheta_N \frac{dM}{d\vartheta_N} + 3M\right) \qquad \gamma_0 = \gamma(r_0)\,,\ \theta_N = \frac{d\theta}{dz}$$

Final step: from shear-deformation to stress-strain: *J2* equivalence

$$\sigma_{eq} = \sqrt{3}\tau \qquad \varepsilon_{eq} = \frac{\gamma}{\sqrt{3}}$$

Numerical models: plasticity

Tests for isotropic model calibration and validation

SAPIENZA UNIVERSITÀ DI ROMA

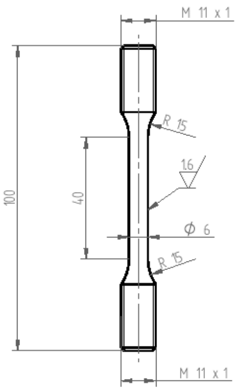

- Tension

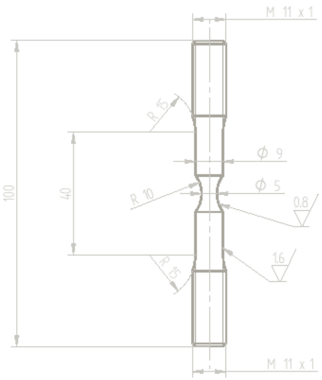

- Round notched

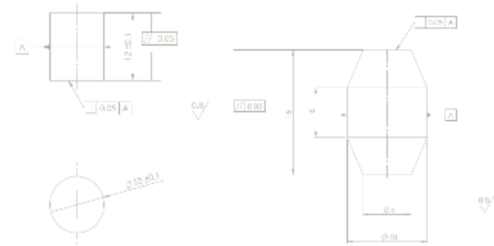

- Compression

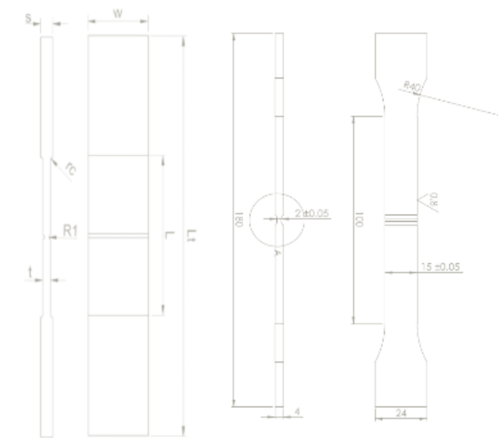

- Plane strain

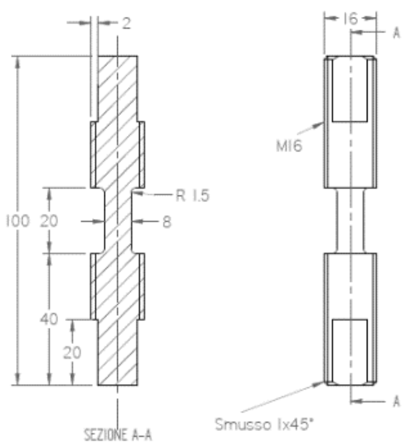

- Torsion

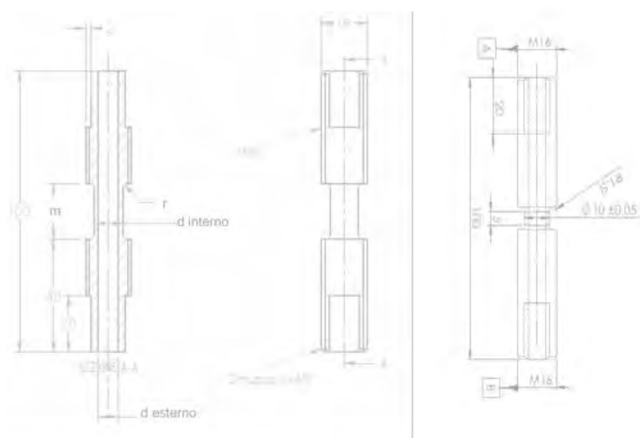

- Tension-Torsion

- Three-point-bend (CSM)

- Cyclic plasticity: Chaboche's Isotropic-kinematic hardening model:

$$F = f(\boldsymbol{\sigma} - \boldsymbol{\alpha}) - \kappa(\alpha) = 0 \longrightarrow F = \frac{3}{2}\left(\sigma'_{ij} - \alpha'_{ij}\right)\left(\sigma'_{ij} - \alpha'_{ij}\right) - \sigma_s^2(\varepsilon_{eq}^p) = 0$$

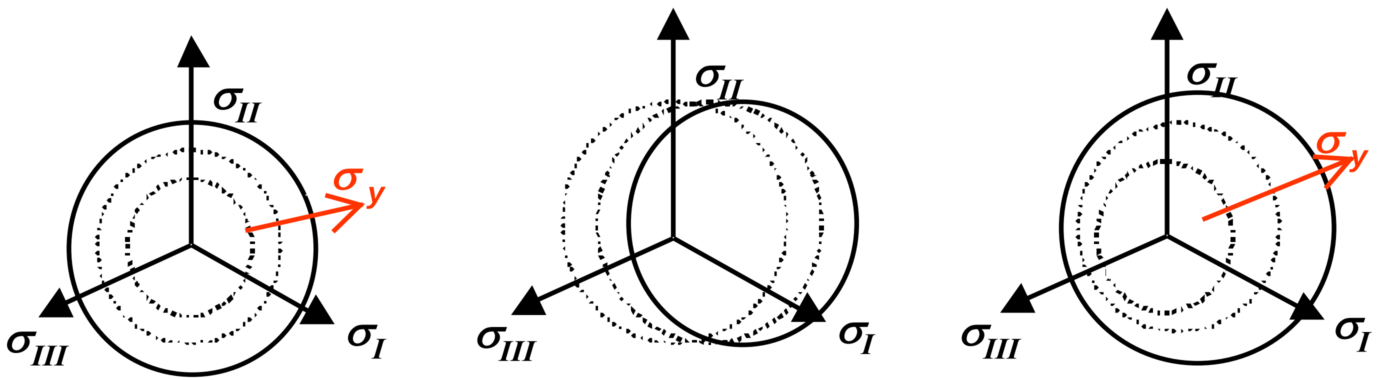

a) Isotropic hardening b) Kinematic hardening c) Combined hardening

Isotropic part of hardening:

$$\sigma_s = \sigma_s^{\ 0} + A(1 - e^{-b\varepsilon_{eq}^p})$$

Kinematic part of hardening:

$$d\alpha = \frac{C}{\sigma_s}(\sigma - a)\, d\varepsilon_p - \gamma\, \alpha\, d\varepsilon_p$$

Material parameters: A, b, C, γ

Inverse methods to identify cyclic plasticity models parameters

SAPIENZA UNIVERSITÀ DI ROMA

- Cyclic plasticity: Tuning of Chaboche's model using inverse methods.

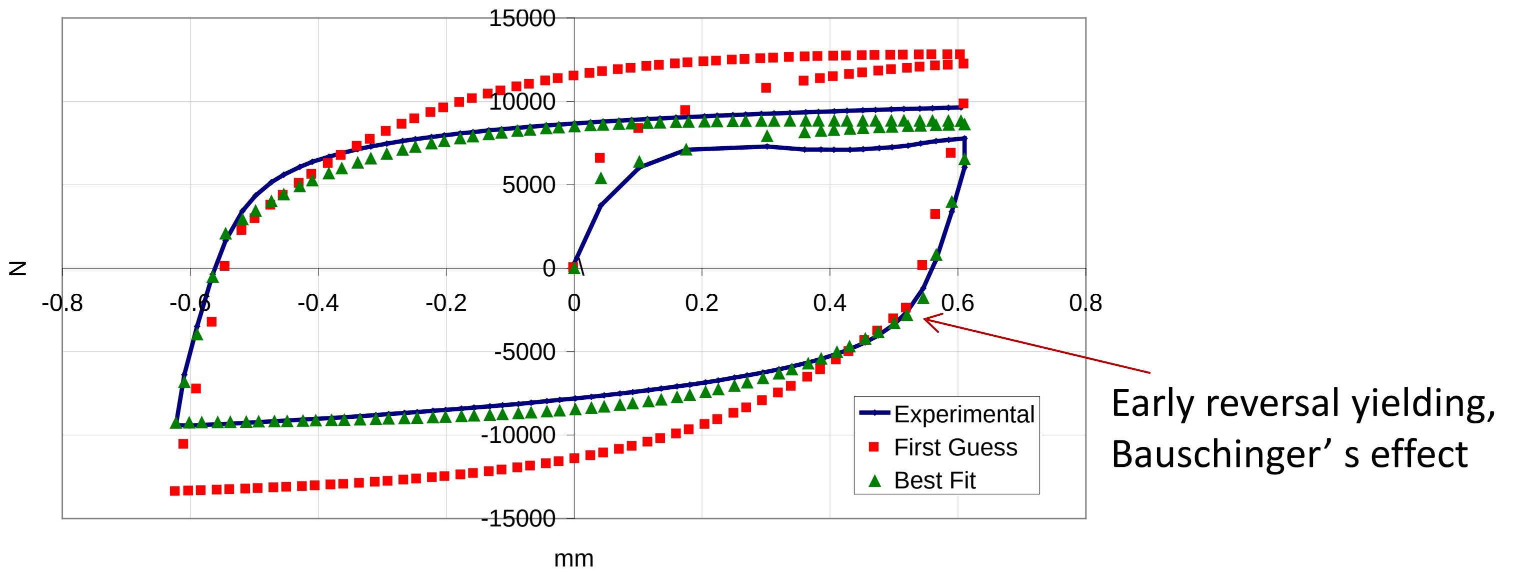

Calibration of Chaboche's model. Applied (per cycle) deformation : $\Delta\varepsilon = 0.05$ m/m.

Broggiato G.B, Campana F, Cortese L, Mancini E (2012). Comparison Between Two Experimental Procedures for Cyclic Plastic Characterization of High Strength Steel Sheets. Journal of engineering materials and technology, vol. 134, p. 63-72, ISSN: 0094-4289, DOI: 10.1115/1.4006919

G.B. Broggiato, F. Campana, L. Cortese. (2008) The Chaboche nonlinear kinematic hardening model: calibration methodology and validation. Meccanica (2008) vol. 43, p. 115-124, ISSN: 0025-6455, DOI: 10.1007/s11012-008-9115-9.

J2-J3 isotropic plasticity model
Theoretical formulation

- Proposal: a new plasticity model, which accounts for the effect of the deviatoric parameter *X*, starting from a Von Mises plasticity.

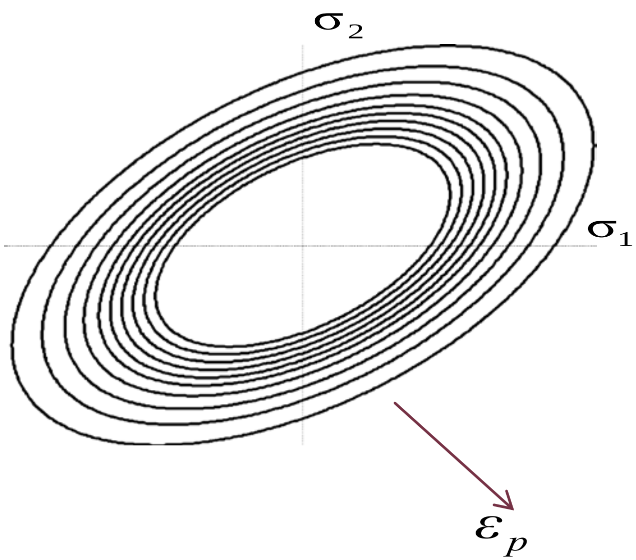

Von Mises *J2* isotropic hardening

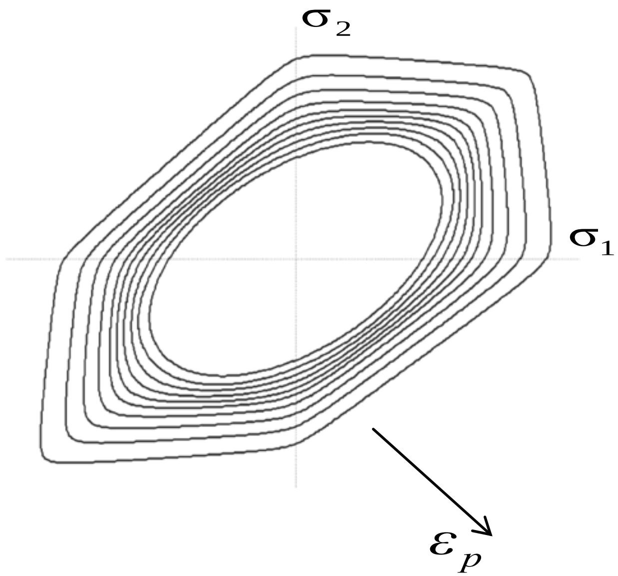

from Von Mises ellipse
to a Tresca-like shape isotropic hardening

- ***(*) Cortese L., Broggiato G.B., Coppola T., Campanelli F., An enhanced plasticity model for material characterization at large strain. Proceedings of the 2013 Annual Conference on Experimental and Applied Mechanics***
- ***Coppola T, Cortese L. Campanelli F. Implementation of a Lode angle sensitive yield criterion for numerical modelling of ductile materials in the large strain range. Proceedings of the XII International Conference on Computational Plasticity (COMPLAS). 3-5 September 2013, Barcelona, Spain.***

- Yield surface (*):

(pressure-insensitive materials)

$$F = \frac{q}{g(X)} - k = 0$$

$$q = \sqrt{3J_2}$$ Equivalent Von Mises stress

$$g(x) = \frac{1}{\cos\left(\beta\frac{\pi}{6} - \frac{1}{3}\arccos(\gamma X)\right)}$$

$$X = \cos(3\theta) = \frac{27}{2}\frac{J_3}{q^3}$$ Lode parameter

θ Lode angle

$\beta \in [0;2]$, $\gamma \in [0;1)$ Material parameters

Uniaxial tensile stress:

$$k = \frac{\sigma(\varepsilon^p)_{Tens}}{g(X=1)}$$

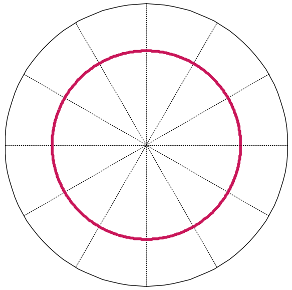

$\beta = 1$
$\gamma = 0$

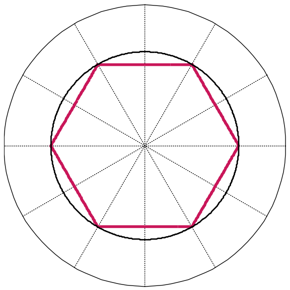

$\beta = 1$
$\gamma = 1$

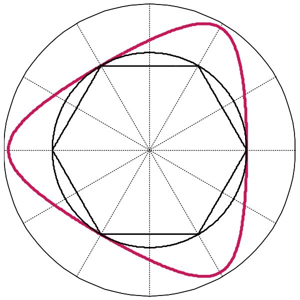

$\beta = 0$
$\gamma = 0.8$

- Stress state related definitions.

Hydrostatic pressure:

$$\sigma_H = \frac{1}{3}\left(\sigma_{xx} + \sigma_{yy} + \sigma_{zz}\right) = \frac{1}{3}\left(\sigma_1 + \sigma_2 + \sigma_3\right)$$

Stress tensor decomposition, total and deviatoric stress tensors:

$$\sigma_{ij} = p\delta_{ij} + s_{ij}$$

$$\bar{\bar{\sigma}} = \begin{bmatrix} \sigma_{xx} & \sigma_{xy} & \sigma_{xz} \\ \sigma_{yx} & \sigma_{yy} & \sigma_{yz} \\ \sigma_{zx} & \sigma_{zy} & \sigma_{zz} \end{bmatrix} \qquad \bar{\bar{s}} = \begin{bmatrix} s_{xx} & s_{xy} & s_{xz} \\ s_{yx} & s_{yy} & s_{yz} \\ s_{zx} & s_{zy} & s_{zz} \end{bmatrix}$$

Stress invariants:

$$I_1 = tr\left(\bar{\sigma}\right) = \sigma_{xx} + \sigma_{yy} + \sigma_{zz}$$

$$I_2 = \frac{1}{2}\left(\sigma_{ii}\sigma_{jj} - \sigma_{ij}\sigma j\right) = \sigma_{xx}\sigma_{yy} + \sigma_{yy}\sigma_{zz} + \sigma_{zz}\sigma_{xx} - \sigma_{xy}^2 - \sigma_{yz}^2 - \sigma_{zx}^2$$

$$I_3 = \det\left(\sigma_{ij}\right) = \begin{vmatrix} \sigma_{xx} & \sigma_{xy} & \sigma_{xz} \\ \sigma_{yx} & \sigma_{yy} & \sigma_{yz} \\ \sigma_{zx} & \sigma_{zy} & \sigma_{zz} \end{vmatrix}$$

Deviatoric stress invariants:

$$J_1 = tr\left(\bar{s}\right) = 0$$

$$J_2 = \frac{1}{2} s_{ij}\, s_{ij} = \frac{1}{6}\left[\left(\sigma_1 - \sigma_2\right)^2 + \left(\sigma_2 - \sigma_3\right)^2 + \left(\sigma_3 - \sigma_1\right)^2\right] = \frac{1}{2}\left(s_1^2 + s_2^2 + s_3^2\right)$$

$$J_3 = \det\left(s_{ij}\right) = s_1 s_2 s_3$$

- Triaxiality parameter and its effect on material ductility.

$$T = \frac{\sigma_H}{\sigma_{eq}}$$

$$\left(T = \frac{I_1}{3\sqrt{3J_2}} \right)$$

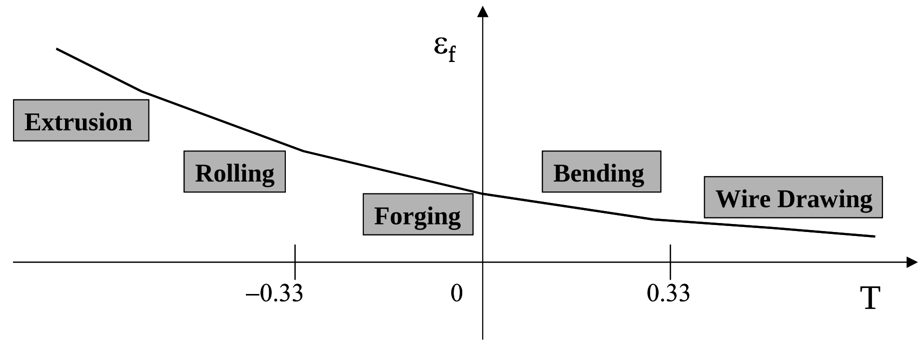

Strain to failure versus triaxiality for critical points of traditional cold forming processes

- Deviatoric parameter

$$X = \frac{27}{2}\frac{J_3}{\sigma_{eq}^3}$$

$$\left(X = \cos 3\theta = \frac{3\sqrt{3}}{2}\frac{J_3}{J_2^{3/2}} \quad (0 \le \theta \le \pi/3) \right)$$

X : Lode parameter, deviatoric parameter
Uniaxial tension -> *X*=1
Pure shear -> *X*=0
Uniaxial compression -> X=-1

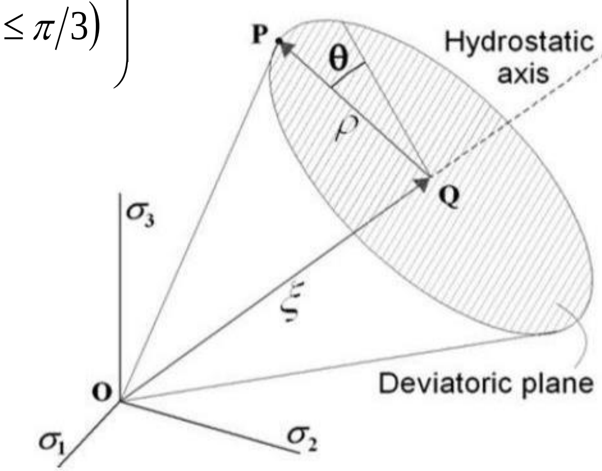

The deviatoric parameter in the principal stress space

- Models with *J2* and *J3* dependence:

$$D = \int_0^{\varepsilon_f^*} \Gamma(T, X)\, d\varepsilon_f$$

$$T = \frac{\sigma_H}{\sigma_{eq}} \qquad X = \frac{27}{2}\frac{J_3}{\sigma_{eq}^3}$$

Under **proportional or quasi-proportional loading conditions** using averaged damage parameters:

$$T_{av} = \frac{1}{\varepsilon_f}\int_0^{\varepsilon_f} T(\varepsilon)\, d\varepsilon_p \qquad X_{av} = \frac{1}{\varepsilon_f}\int_0^{\varepsilon_f} X(\varepsilon)\, d\varepsilon_p$$

Fracture locus:

$$\varepsilon_f = \Gamma^{-1}(T, X)$$

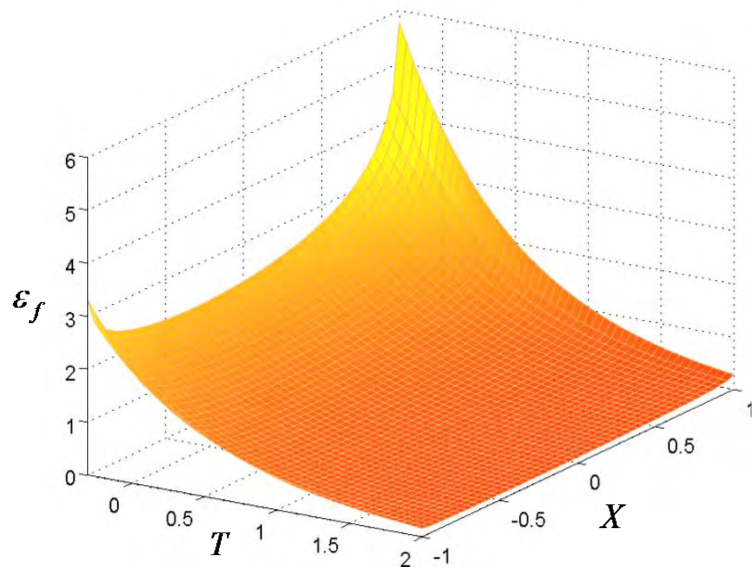

The same operation could have been done for models relying on *T* only

- Coppola-Cortese

$$D = \int_0^{\varepsilon_f^*} \frac{f(T)}{\left(\dfrac{G(X)}{G(X=1)}\right)^{\frac{1}{n}}} d\varepsilon_f$$

(*,**)

(Fracture occurs as $D = 1$)

Where:

$f(T) = C_1 e^{C_2 T}$ Triaxiality dependence

$G(X) = \dfrac{1}{\cos\left(\beta \dfrac{\pi}{6} - \dfrac{1}{3}\arccos(\gamma X)\right)}$ Deviatoric function

n exponent of a power law fit of the σ-e curve: $\sigma = A\varepsilon_p^{\ n}$

4 material parameters:

C_1, C_2 — *In f(T)*

β, γ — *In G(X)*

- ***(*) T. Coppola, L. Cortese, P. Folgarait . The Effect of Stress Invariants on Ductile Fracture Limit in Steels". Engineering Fracture Mechanics (2009)***
- ***(**) Cortese L., Coppola T., Campanelli F., Campana F., Sasso. Prediction of ductile failure in materials for onshore and offshore pipeline applications. International Journal of Damage Mechanics 23, 104-123 (2014).***
- ***G.B. Broggiato, F. Campana, L. Cortese. (2007) Identification of Material Damage Model Parameters: an Inverse Approach Using Digital Image Processing. Meccanica (2007), vol. 42, p. 9-17,***

Numerical models: ductile damage prediction

Damage models based on triaxiality and deviatoric parameter

SAPIENZA UNIVERSITÀ DI ROMA

- Cortese-Campanelli-Coppola: use of *J2-J3* plasticity

$$D = \int_0^{\varepsilon_f^*} \frac{f(T)^{n_1/n_X}}{\left(\frac{A_X}{A_1}\frac{G(X=1)}{G(X)}\right)^{1/n_X}} d\varepsilon_p$$

(*)

(Fracture occurs as D = 1)

Proportional loading assumption

⬇

Fracture locus

$$\varepsilon_f = \left(\frac{1}{C_1} e^{-C_2 T}\right)^{\frac{n_1}{n_X}} \left(\frac{A_1}{A_X}\frac{G(X)}{G(X=1)}\right)^{\frac{1}{n_X}}$$

- ***(*) Cortese L., Coppola T., Campanelli F., Broggiato G.B., A J2-J3 Approach in Plastic and Damage Description of Ductile Materials. Int. J. of Damage Mechanics, 2015.***
- ***Coppola T, Cortese L, Guarnaschelli C, Salvatori I. (2013). Application of ductile damage concepts in the evaluation of material formability during screw head cold forming. 12th International Conference on Fracture and Damage Mechanics (FDM). Alghero, Sardinia, Italy. September 17-19, 2013.***

Numerical models: ductile damage

Multiaxial tests for models calibration/validation

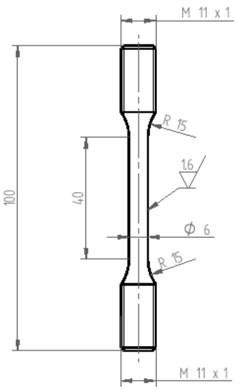

❑ Tension

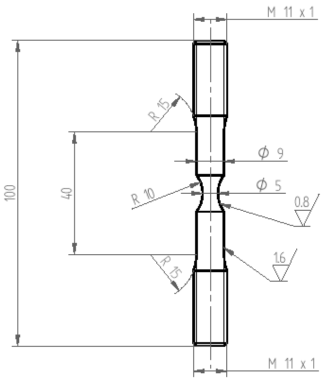

❑ Round notched

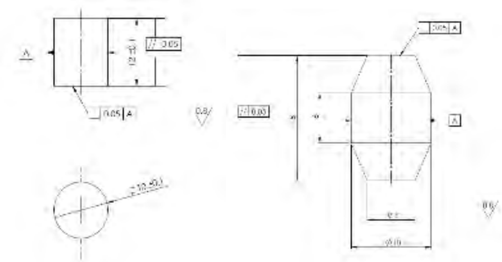

❑ Compression

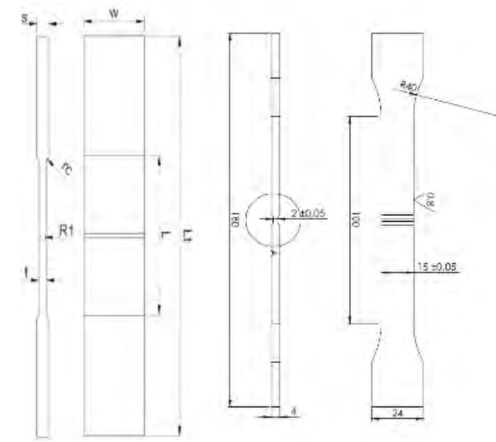

❑ Plane strain

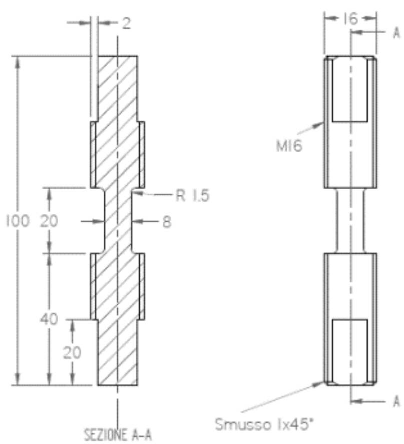

❑ Torsion

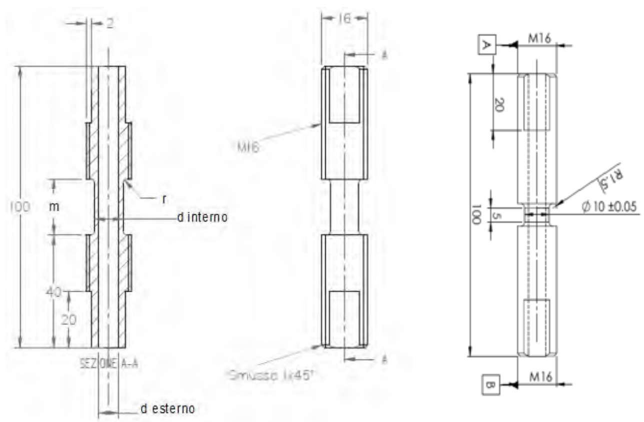

❑ Tension-Torsion

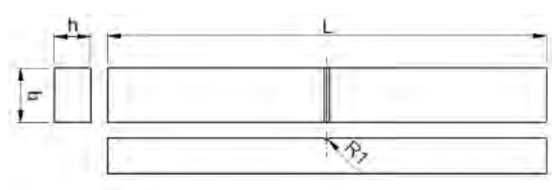

❑ Three-point-bend (CSM)

- Fracture locus localization of different experimental tests.

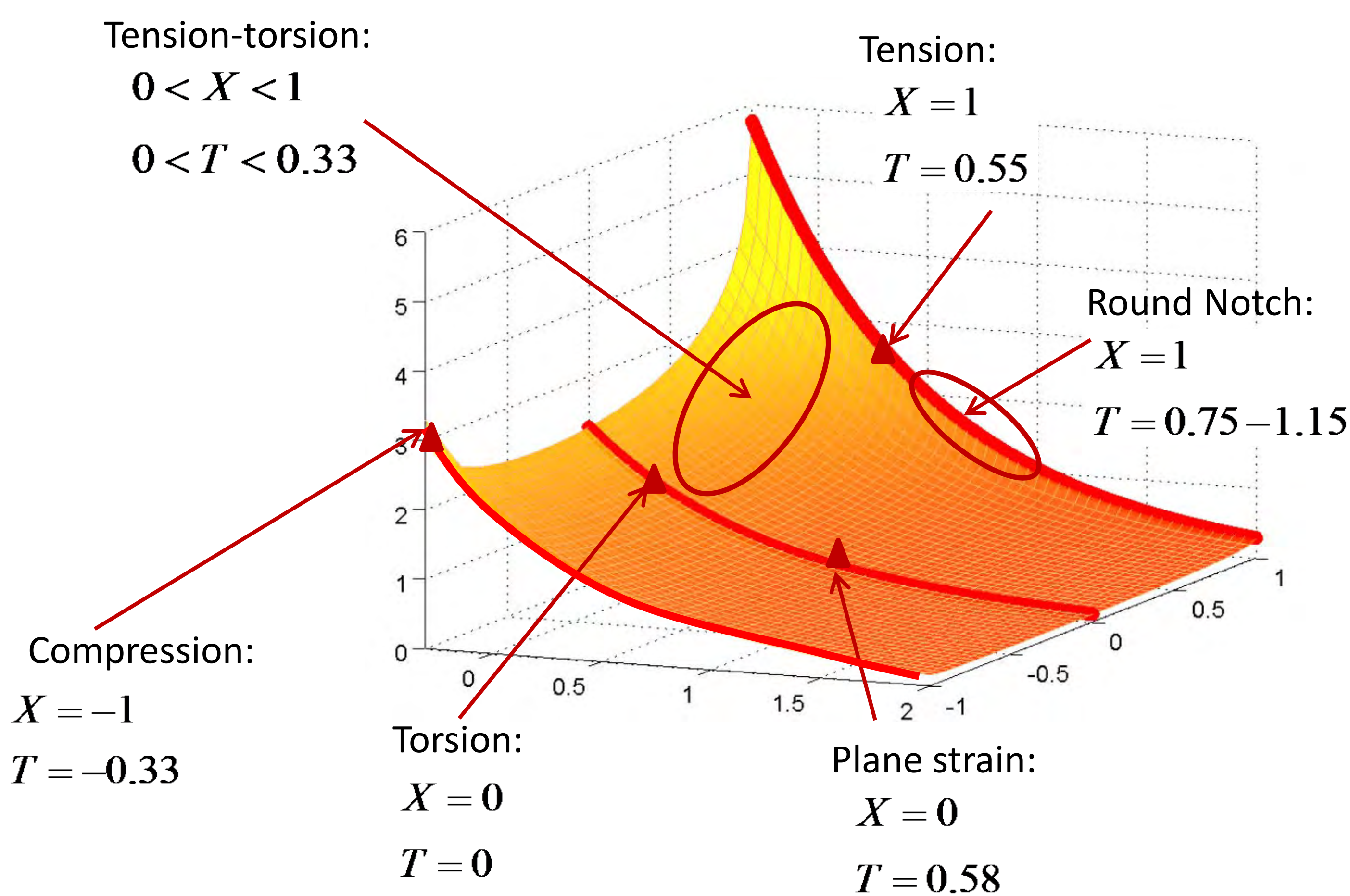

Calibration results

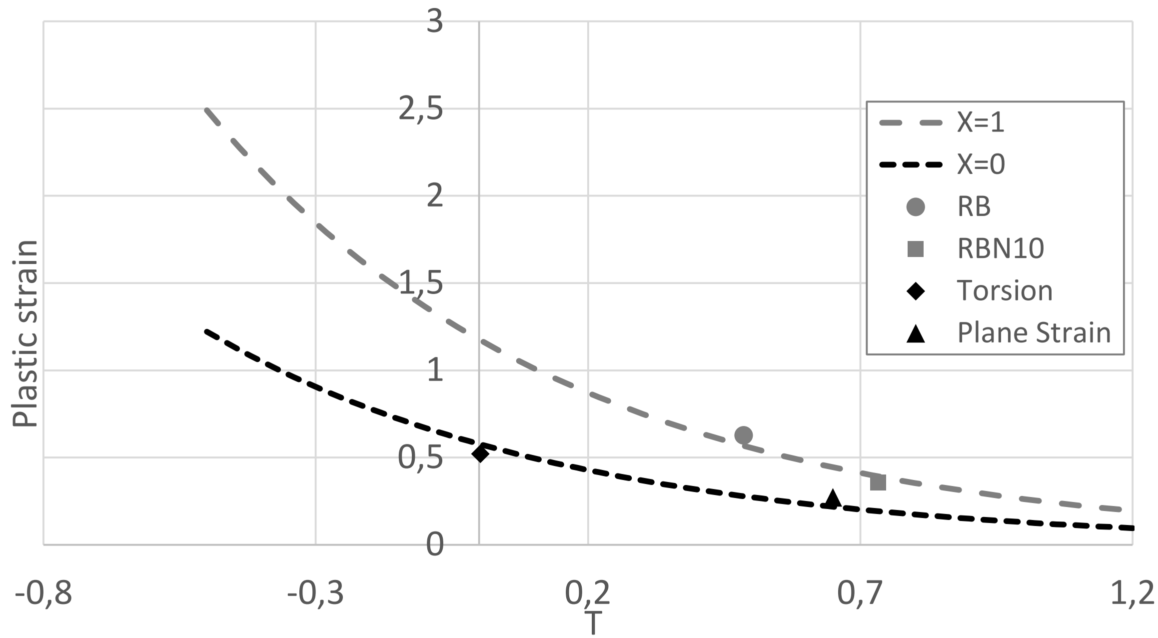

Calibration based on minimum number (4) of tests:

- Tension
- RNB 10
- Torsion
- Plane strain

Values of *T, X* and ε_f at critical points.

	RB	*RNB10*	*Torsion*	*Plane Strain*
$T_{average}$	0.54	0.74	0.00	0.66
$X_{average}$	1.00	1.00	0.00	0.00
$\varepsilon_{fracture}$	0.62	0.35	0.41	0.33

- ***L. Cortese, F. Nalli, T. Coppola, G.B. Broggiato. (2015). An effective experimental-numerical procedure for damage assessment of Ti6Al4V. SEM 2015 Annual Conference and Exposition on Experimental and Applied Mechanics, Costa Mesa, Costa Mesa, California, USA, June 8-11, 2015.***

- Non linear damage enhancement proposal

$$\sum\left(\frac{n}{N}\right)^k \longleftrightarrow \int\left(\frac{d\varepsilon_p}{\varepsilon_f}\right)^k$$

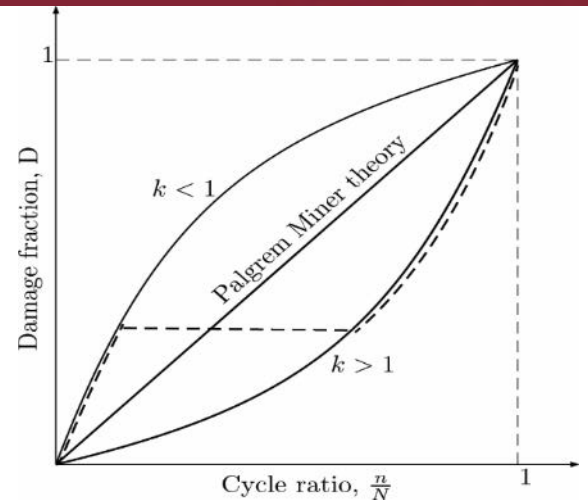

- Polimorphic formulation, working with linear damage models

$$D = \left(\frac{\varepsilon_p}{\varepsilon_f}\right)^{\frac{m}{\varepsilon_f{}^{mm}}}$$

$$\varepsilon_f = \varepsilon_f(T, X)$$

$$D = \int_0^{\varepsilon_f{}^*} \frac{m}{\varepsilon_f{}^{mm+1}}\left(\frac{\varepsilon_p}{\varepsilon_f}\right)^{\frac{m}{(\varepsilon_f{}^{mm})}-1} d\varepsilon_p$$

L. Cortese, F. Nalli, M. Rossi (2016) A nonlinear model for ductile damage accumulation under multiaxial non-proportional loading conditions. International Journal of Plasticity vol. 85, October 2016.

Numerical models: ductile damage

Nonlinear damage model enhancement

SAPIENZA
UNIVERSITÀ DI ROMA

- Non proportional tension-torsion tests

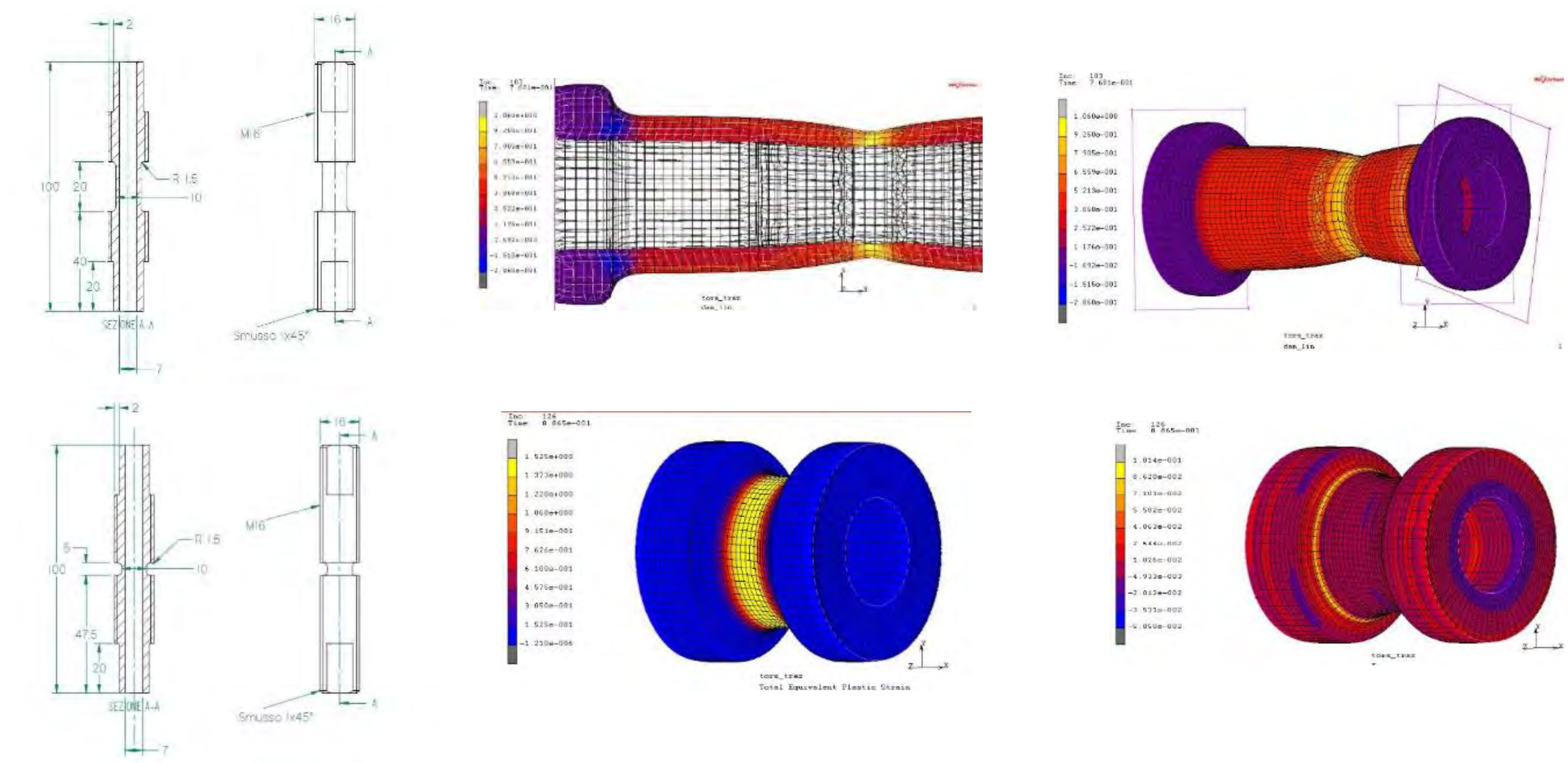

3D models reproducing the experiments, with adaptive remeshing features

- Non proportional tension-torsion tests.

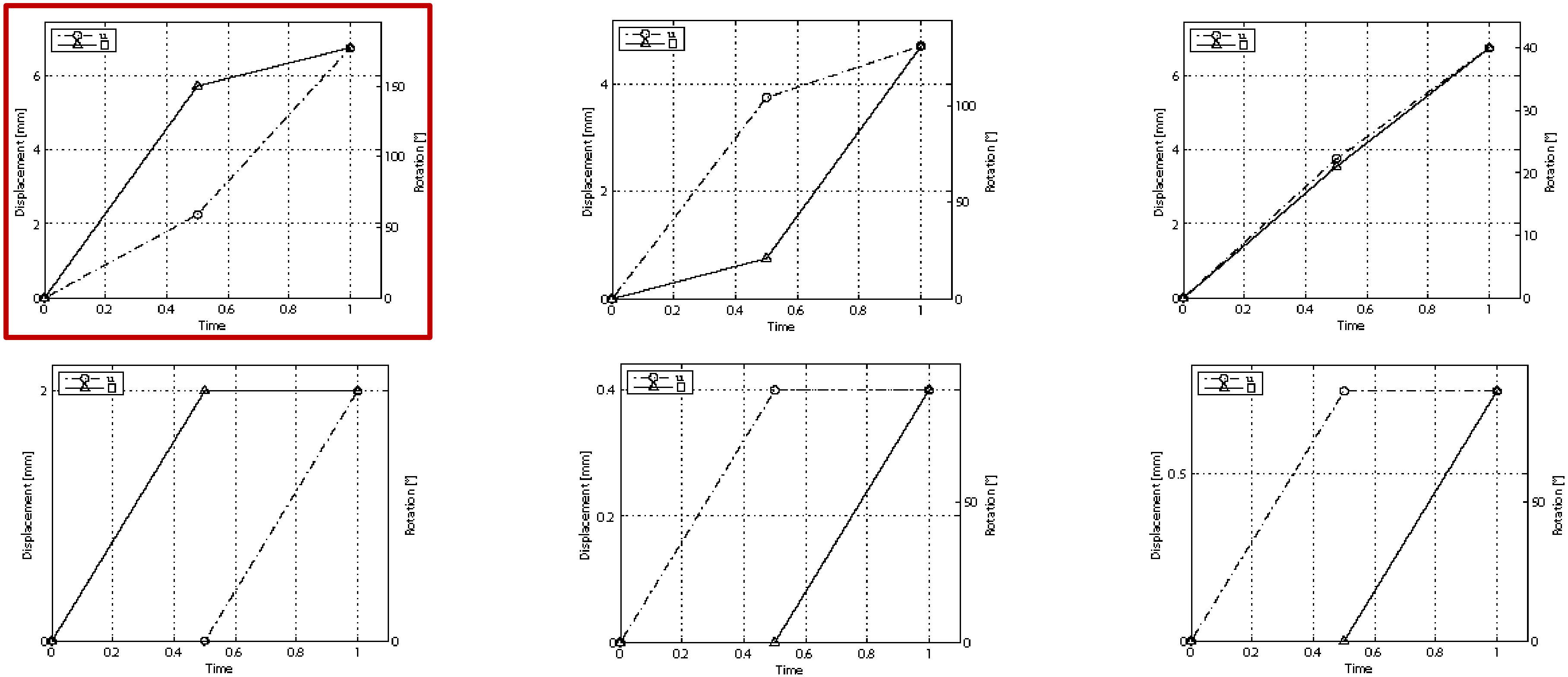

Double proportional paths, designed by FE analysis

- Damage prediction for all tests: linear-nonlinear comparison

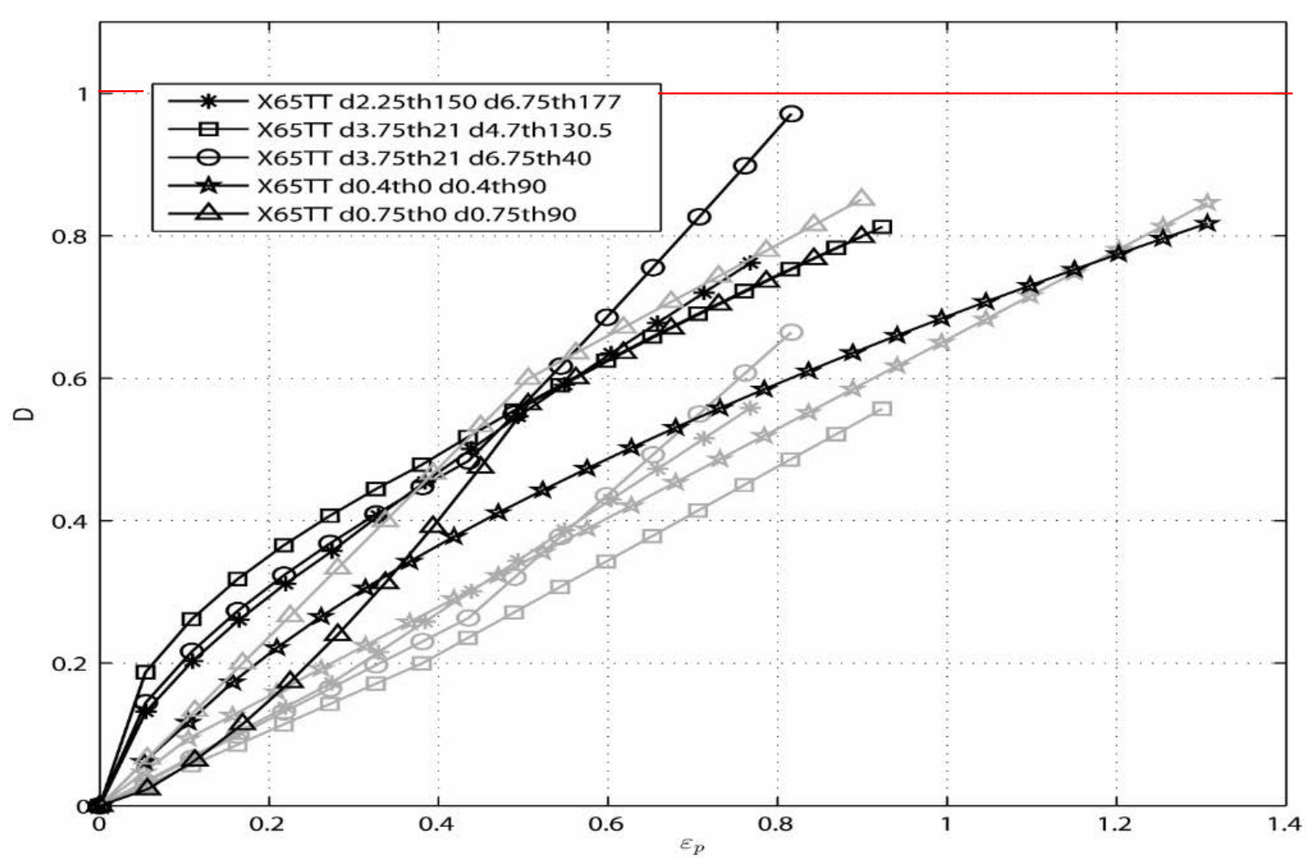

Damage accumulation with equivalent plastic strain for all double proportional paths: linear and non linear estimation

Example, at laboratory level: tensile test of a round notch bar

- Structural integrity: plasticity and damage models in FE analysis should predict the proper material elasto-plastic behaviour and final failure. This under "any" loading condition.

Simple example: numerical simulation of a tensile test on a round notched specimen. Numerical models should be able to describe the deformation and the exact moment of failure

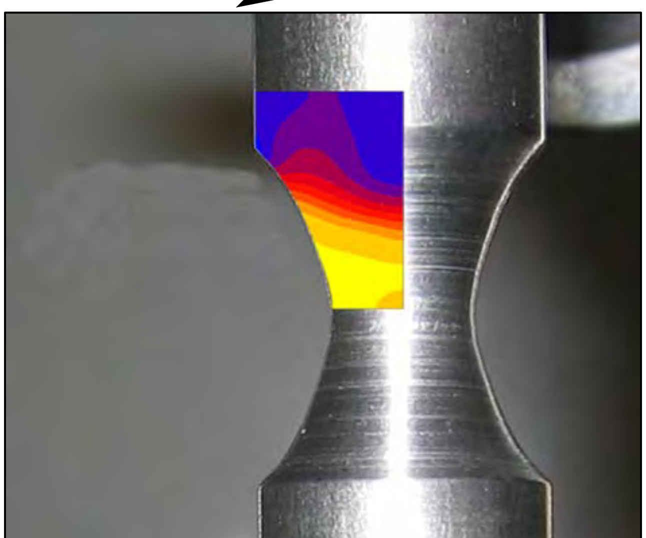

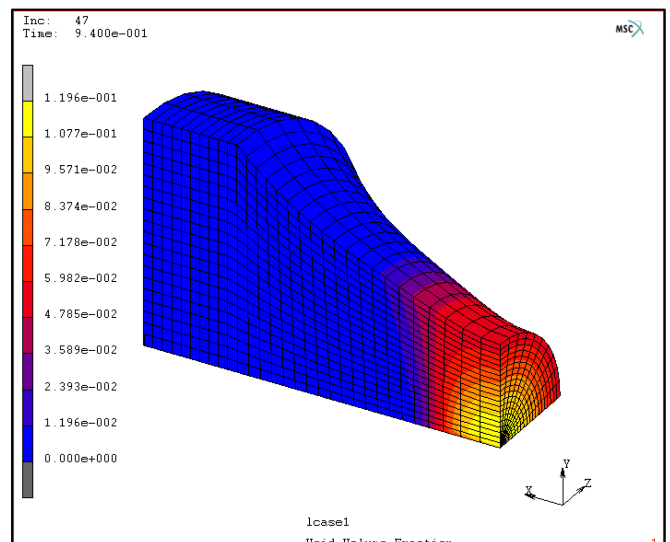

- Offshore pipelines installation techniques: S-lay and J-lay

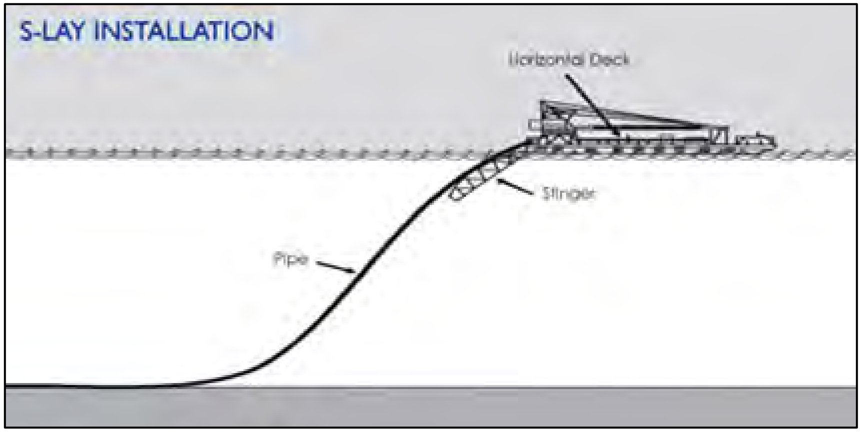

Source: www.pbjv.com.my

Welding station and lifting crane on board. Pipes assembled one section at a time and laid down by means of a guide (stinger).

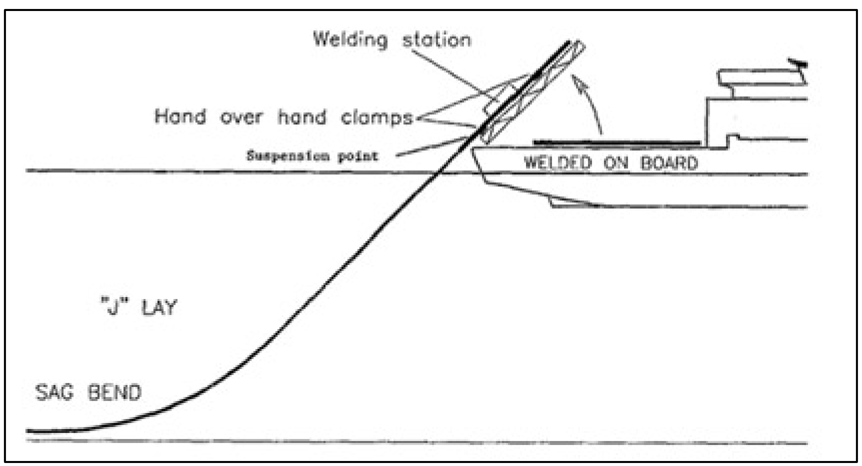

Source: www.technip.com

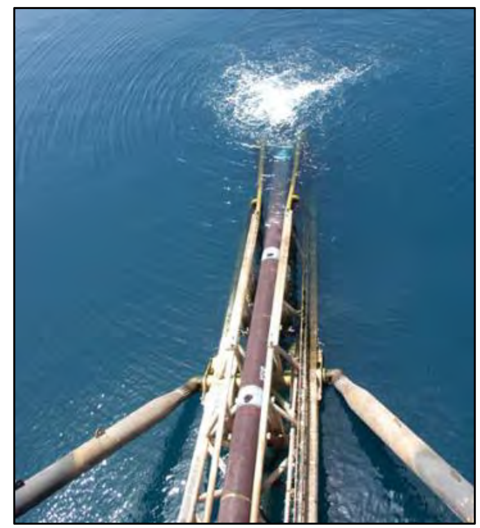

Source: www.nord-stream.com

- Offshore pipelines installation techniques: reel-lay

Reel barges contain a vertical or horizontal reel that the pipe is wrapped around. Reel barges are able to install both relatively small diameter pipe and flexible pipes. Pipe welding is performed onshore.

Pipeline steels undergo plastic deformation in the laying process, leading to significant residual stresses. During service, materials must withstand those, in addition to the stressed due to the nominal loading conditions (oil or gas pressure, hydrostatic water pressure, …). Damage models could help in stating whether new materials could be suited for such applications before investing, risking..

Digital image correlation (DIC) applied to advanced material characterization

- 2D white-light speckle image correlation techniques for full-field surface displacement and strain measurement
- Application of DIC to material characterization and numerical model robust calibration
- DIC applied to the structural characterization of welded joints (using different welding techniques, for automotive applications, particularly tailored welded blanks

- Grid methods

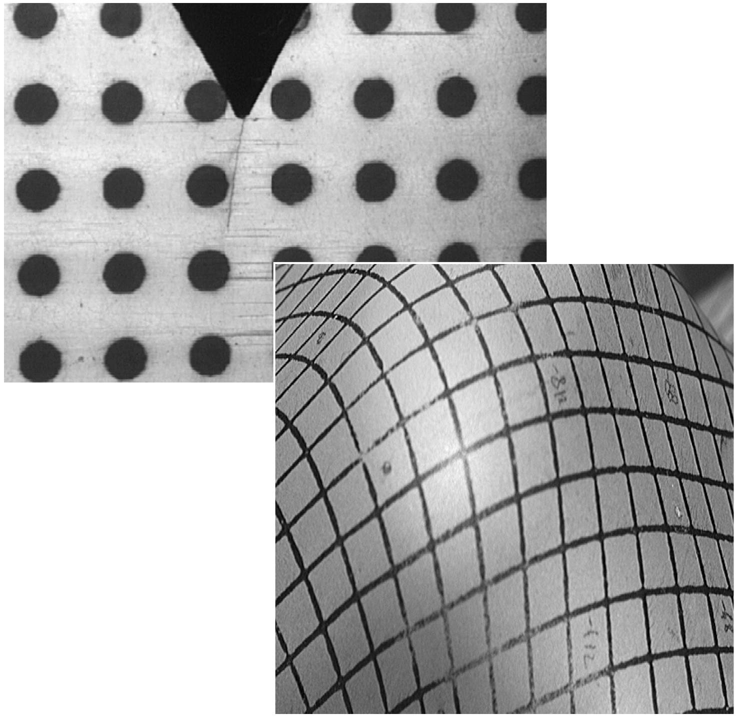

- Speckle-image based methods

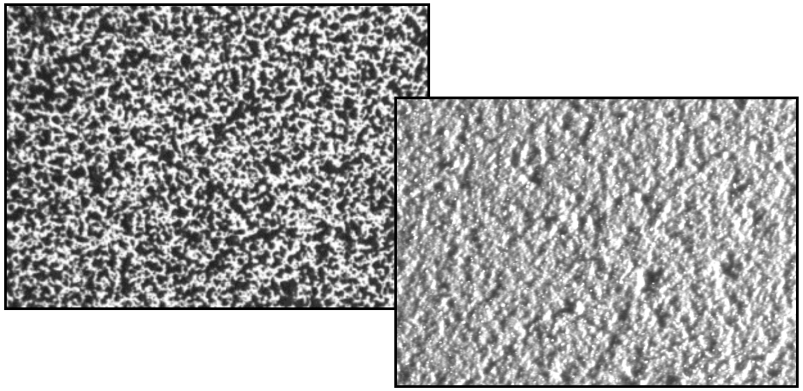

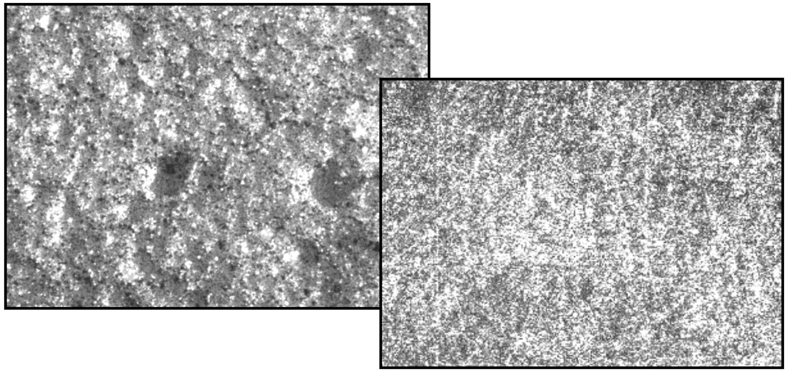

- Non linear fitting among image sets (global approach for full-field analysis)

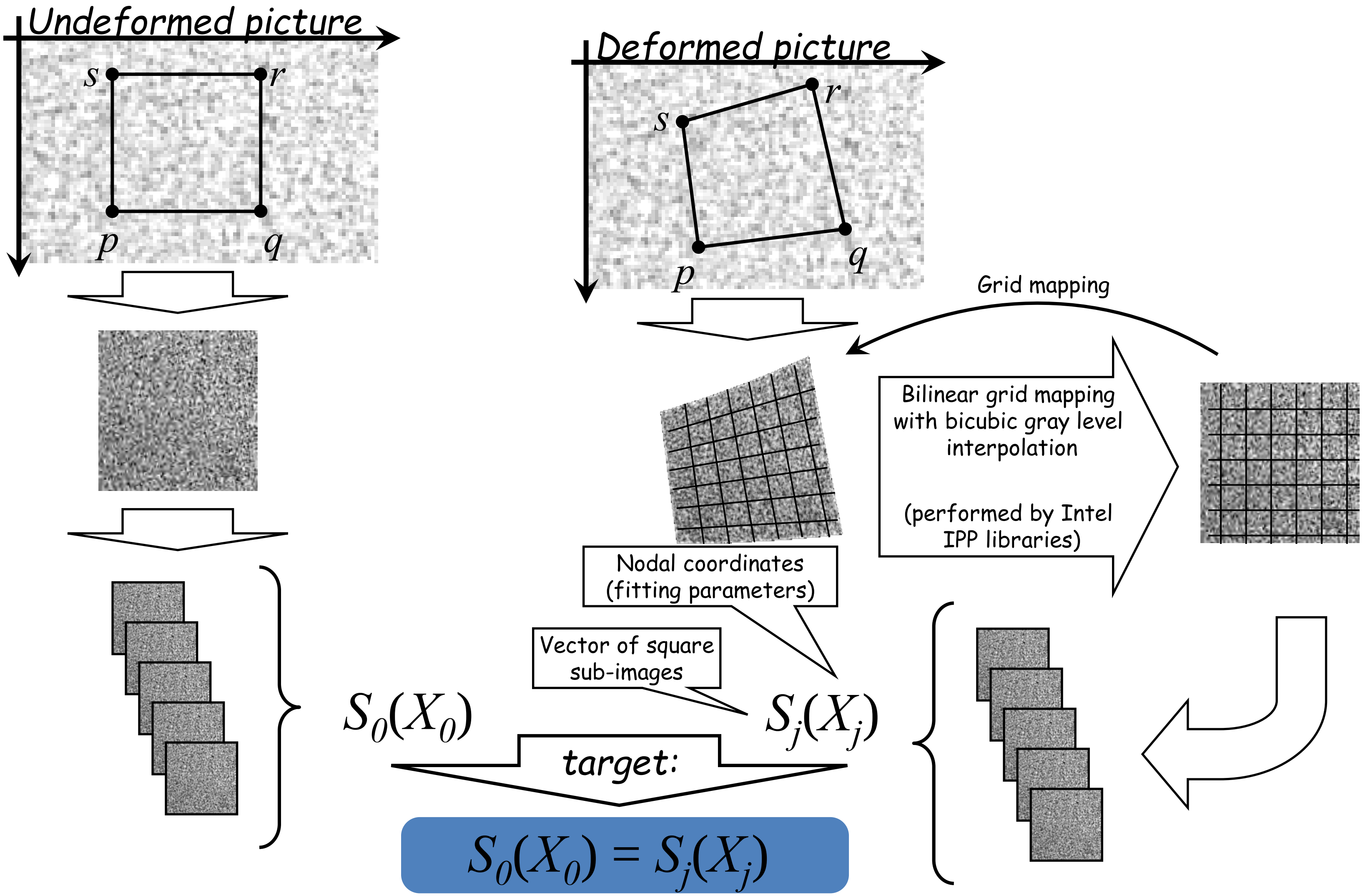

- Method application main steps:

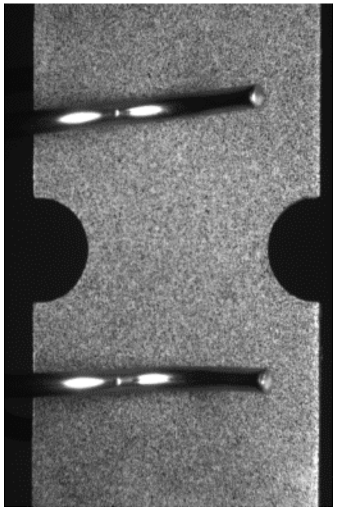

Reference image
(first picture of the sequence)

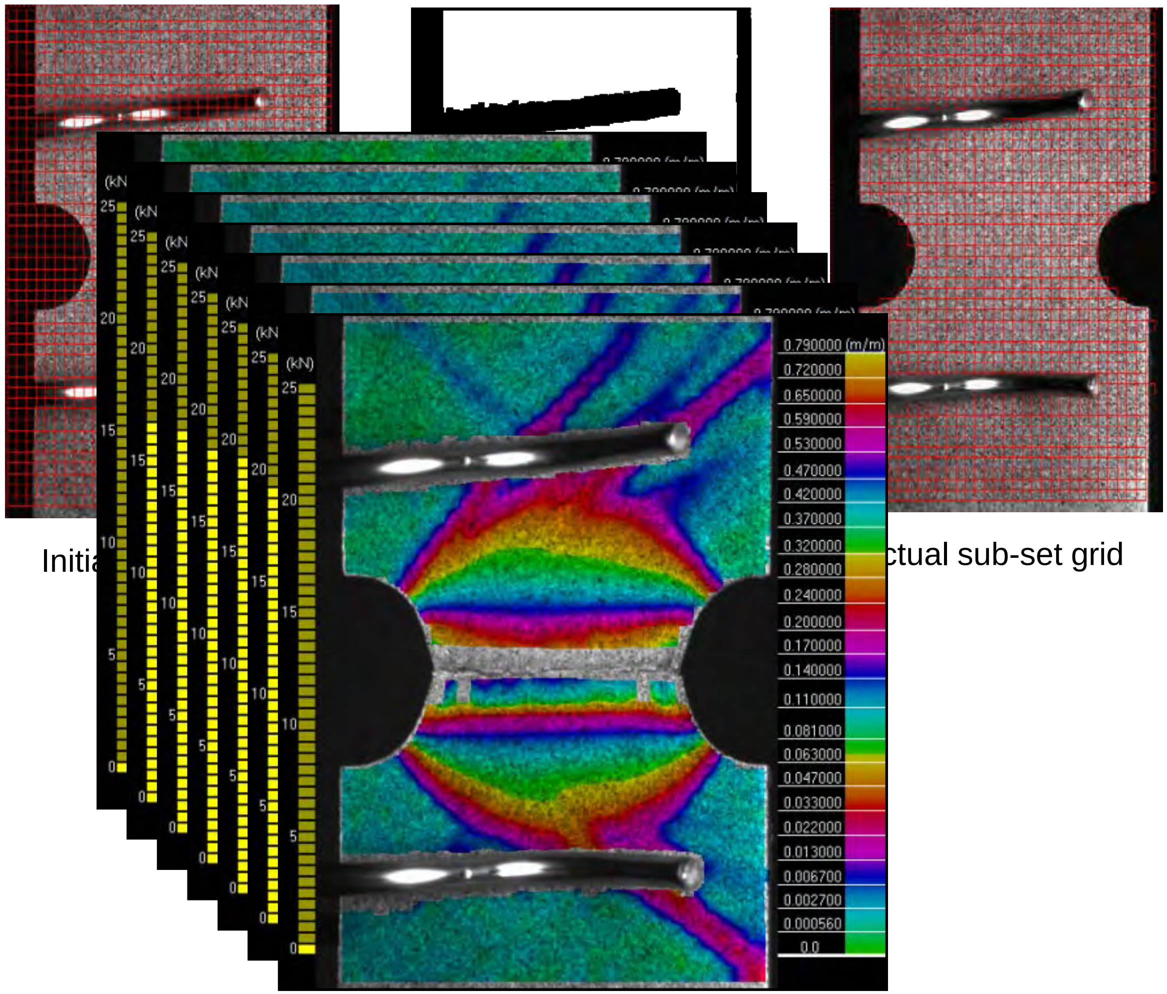

Initi

ctual sub-set grid

Digital image analysis

2D white-light speckle image

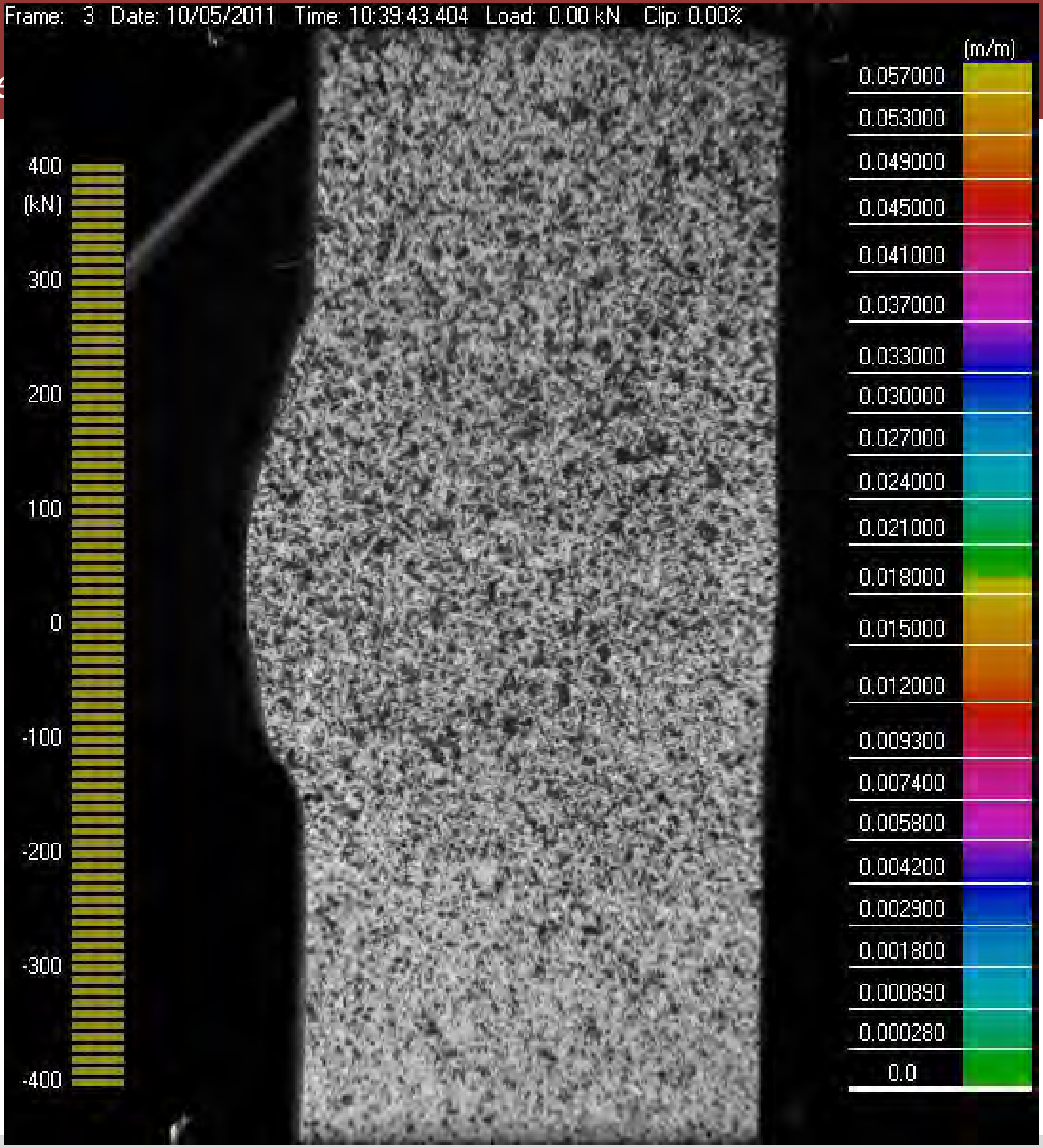

- 2D white light speckle digital image analysis

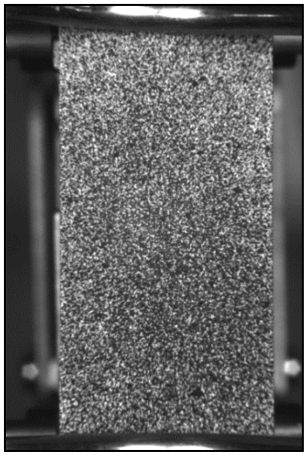

ε = 0.02 m/m

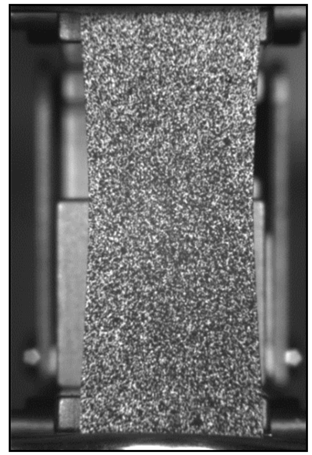

ε_{max} = 0.4 m/m

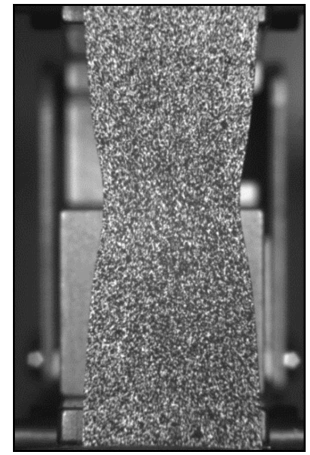

ε_{max} = 0.7 m/m

Flat specimens sprayed with black speckles on a white base paint

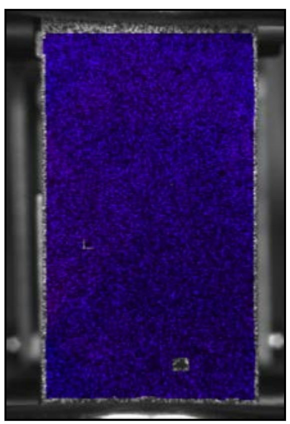

ε = 0.02 m/m

ε_{max} = 0.4 m/m

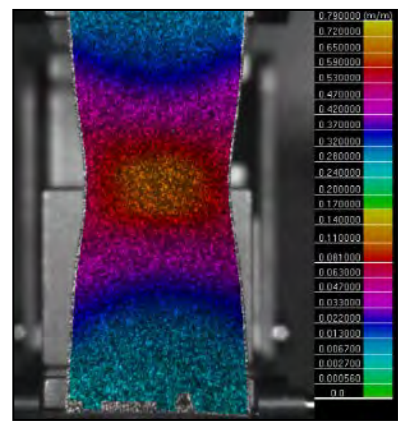

ε_{max} = 0.7 m/m

Strain field contour maps (components or equivalent)

- Joint characterization: tensile tests on hourglass laser welded specimens

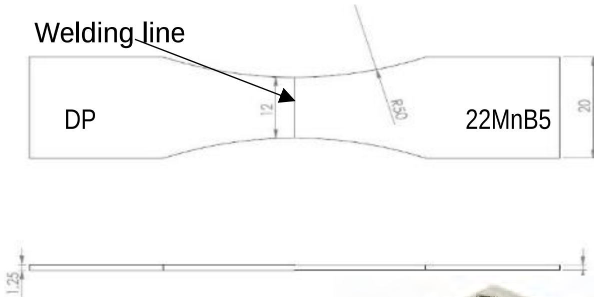

Property	DP Dual Phase	22MnB5 Hot stamping boron steel
σ_y [MPa]	470	1050
σ_r [MPa]	690	1440
Elongation at fracture [%]	19	5

Camera
Pixelink A781
CMOS Sensor
3000 x 2208 px
Lens
Telecentric
1:1 magnification ratio

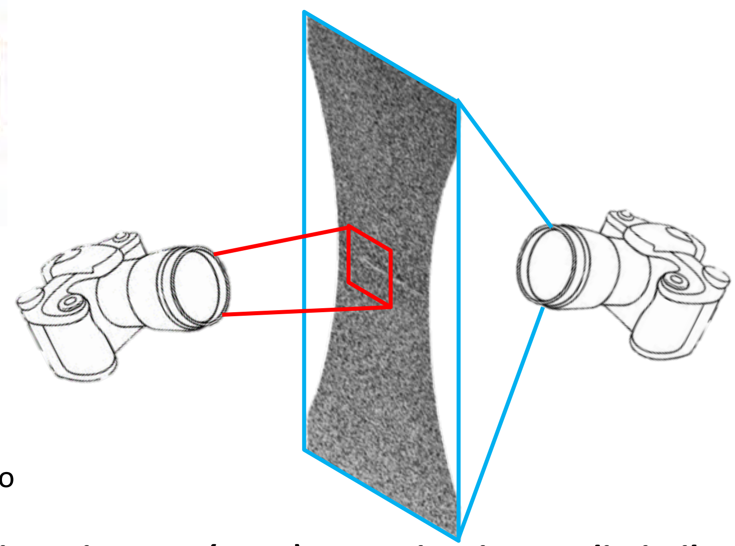

Camera
Nikon D7000
CMOS Sensor
4928 x 3264 px

Lens
Nikkor 60mm macro

- ***Rossini M, Russo Spena P, Cortese L, Matteis P, Firrao D. (2015). Investigation on dissimilar laser welding of advanced high strength steel sheets for the automotive industry. Materials Science and Engineering A, 628, pp. 288-296.***
- ***Broggiato G.B, Cortese L, Nalli F, Russo Spena P. (2015). Full Field Strain Measurement of Dissimilar Laser Welded Joints. Procedia Engineering, Volume 109, 2015, Pages 356–363.***

Digital image analysis
Application to laser welding of dissimilar High Strength Steel Alloys

SAPIENZA
UNIVERSITÀ DI ROMA

- Experimental results

Total equivalent strain

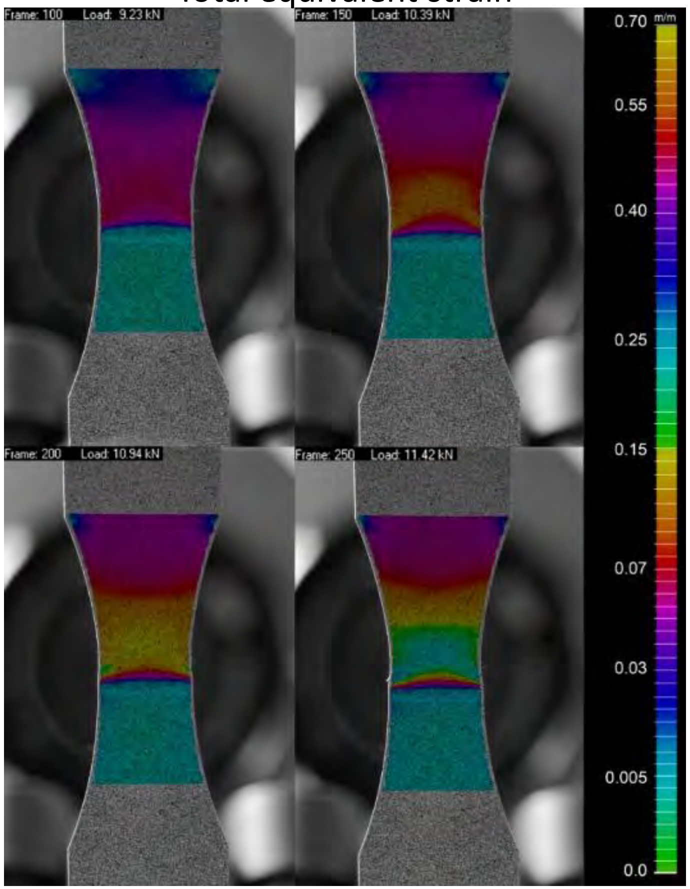

Through thickness strain

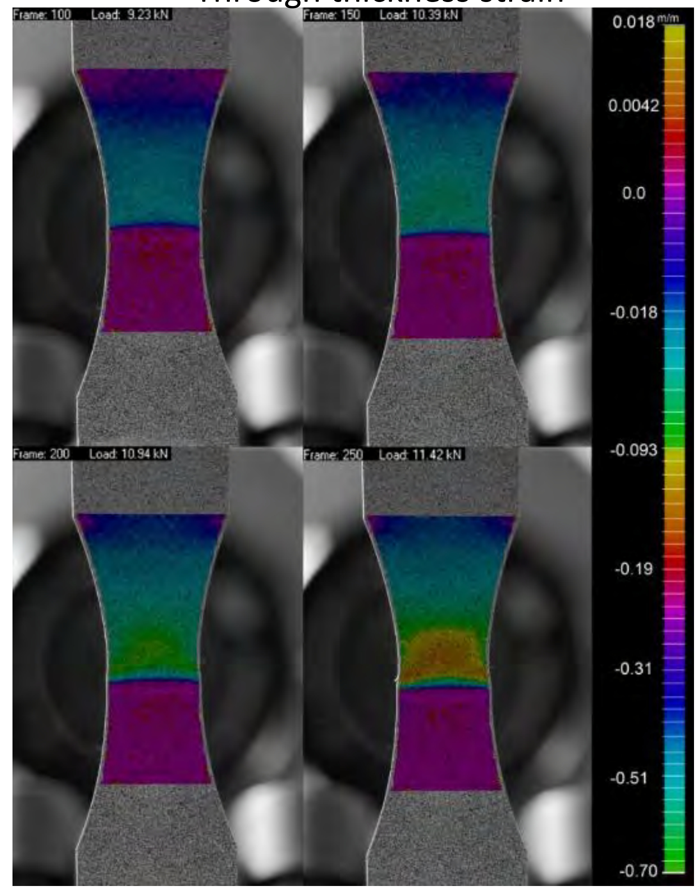

Acquisition camera: SLR Nikon D7000. Grid dimension: 0.5 mm

Digital image analysis

Application to laser welding of dissimilar High Strength Steel Alloys

SAPIENZA
UNIVERSITÀ DI ROMA

- Experimental results

Different magnification levels allows to retrieve the full-field displacement and strain on the whole specimen and increased resolution where higher gradients are expected.

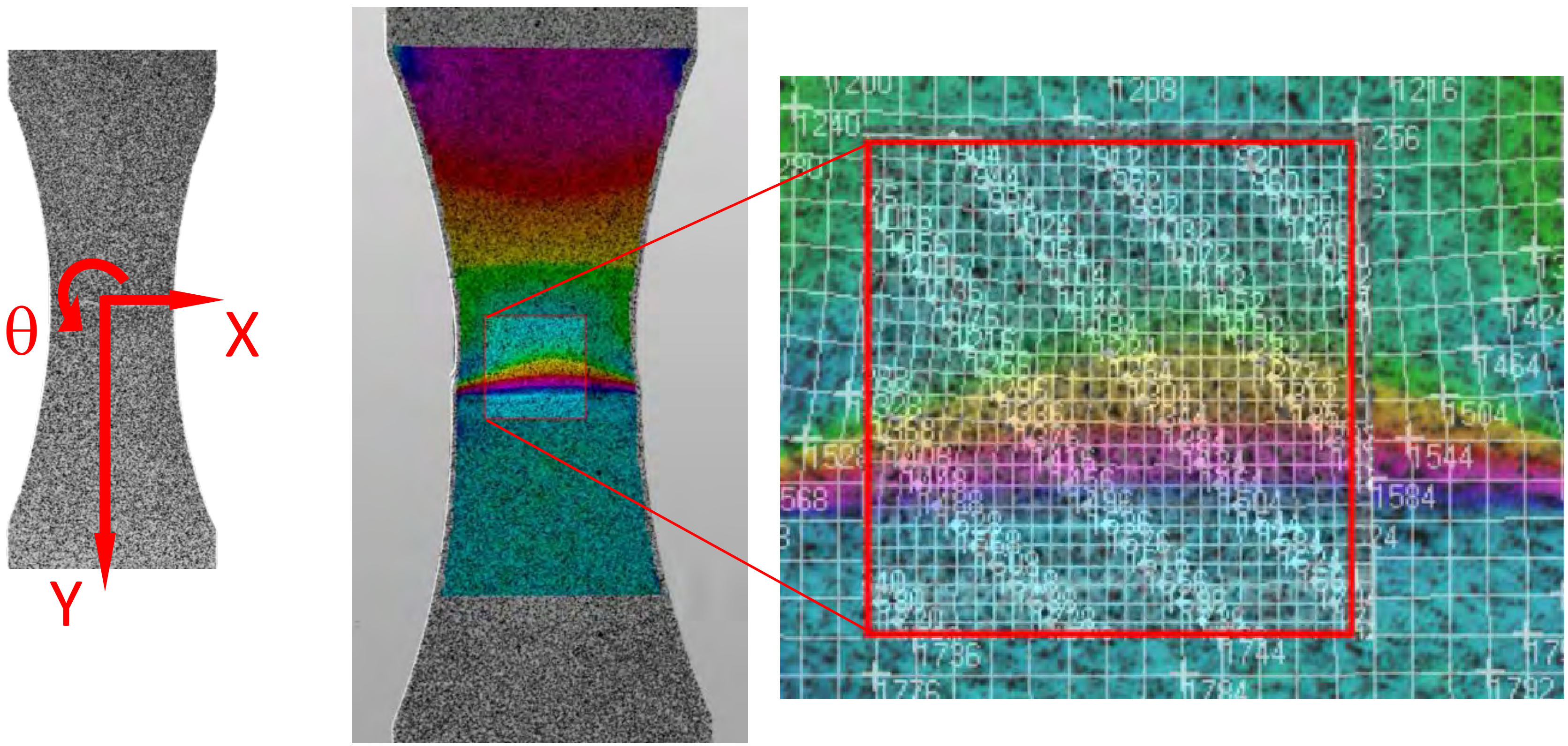

G.B. Broggiato, L. Cortese, F. Nalli

Department of Mechanical and Aerospace Engineering

Experimental-numerical techniques applied to the restoration of cultural heritage

- Antonello da Messina: “L’annunciazione”
- Michelangelo Caravaggio: “La resurrezione di Lazzaro”
- Raffaello Sanzio: “Il Cartone preparatorio per la Scuola di Atene”

- Stress state evaluation in canvas: investigated artworks

- Antonello da Messina:
  "L'Annunciazione"

- Caravaggio:
  "La Resurrezione di Lazzaro"

- Raffaello:
  preparatory drawing of «The School of Athens»

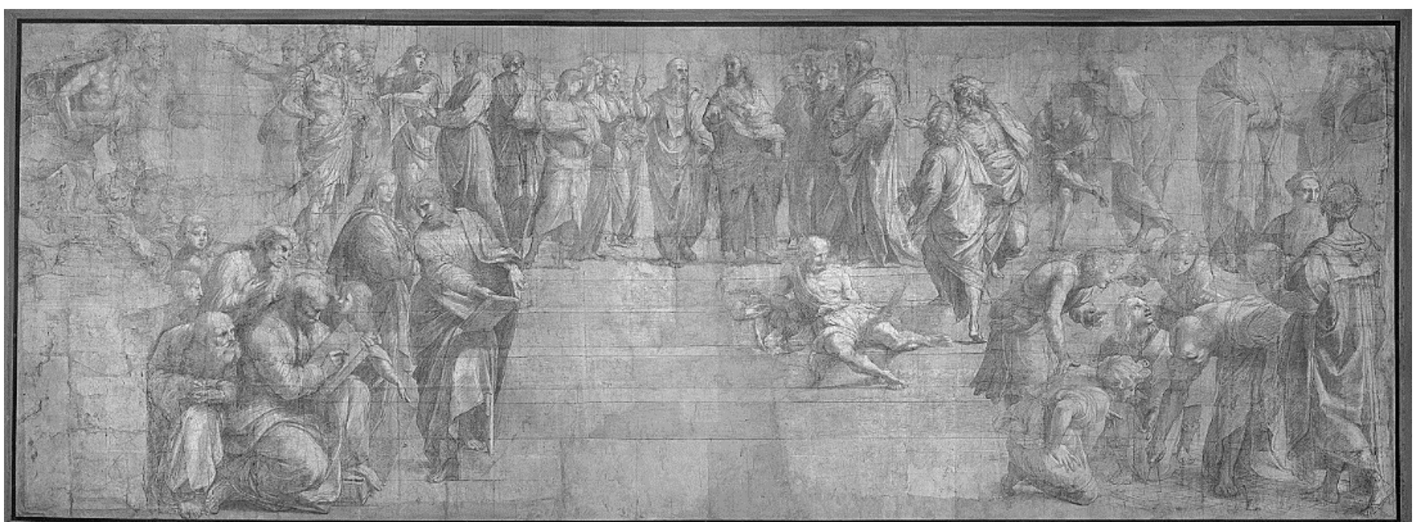

From: «Tecniche numeriche e sperimentali dell'ingegneria meccanica applicate alla conservazione dei beni culturali». Broggiato, Cortese, Santucci, Torre. Modelli matematici nella conservazione e valorizzazione dei beni culturali. Accademia Nazionale dei Lincei, 15 – 16 dicembre 2015

The «Cartone» of Raffaello

Preparatory drawing for the fresco:
«La scuola di Atene» of Raffaello Sanzio

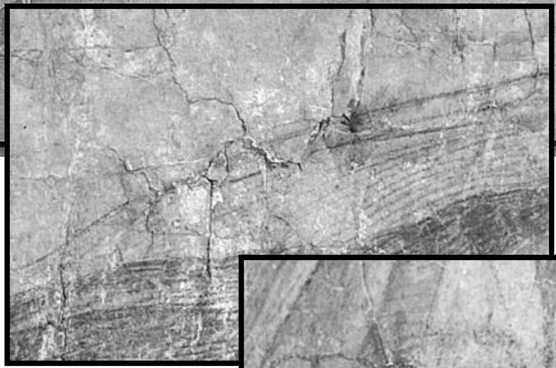

- Structural details

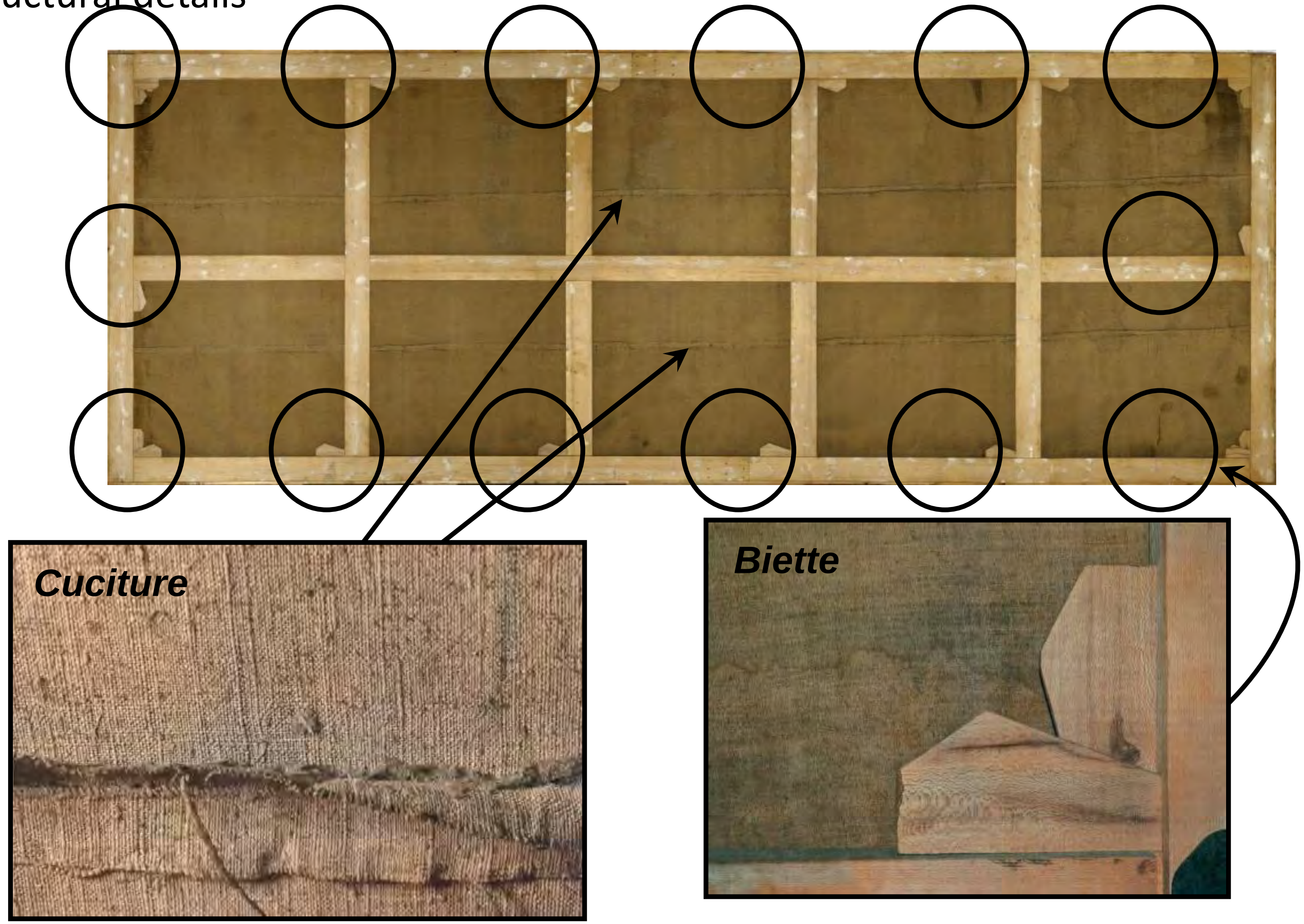

❑ Mechanical experimental setup

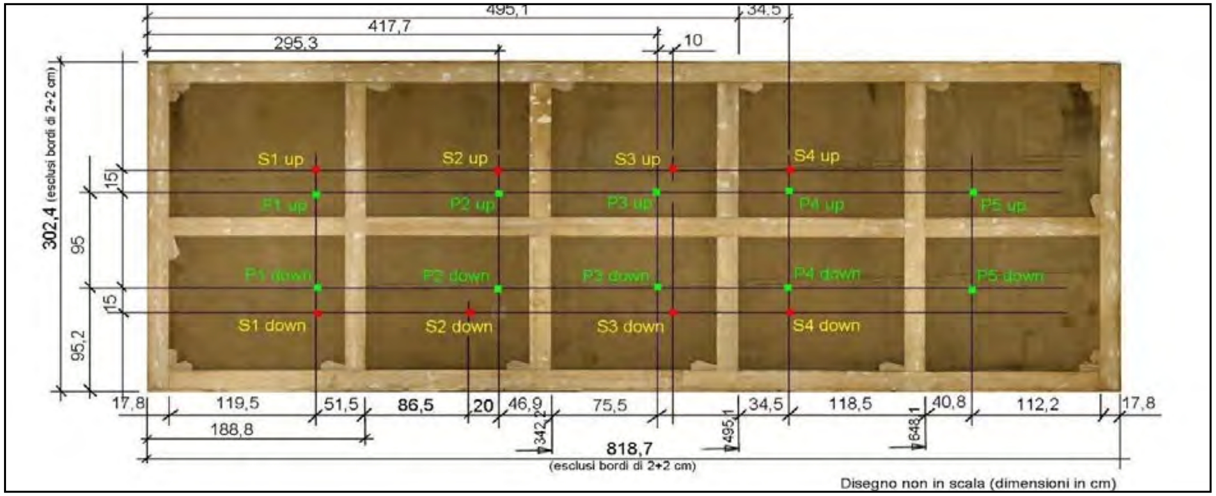

Actuation points (S) and Displacement transducers (P)

Linear actuator, manual. Applied loads: 1N, 2N, 3N

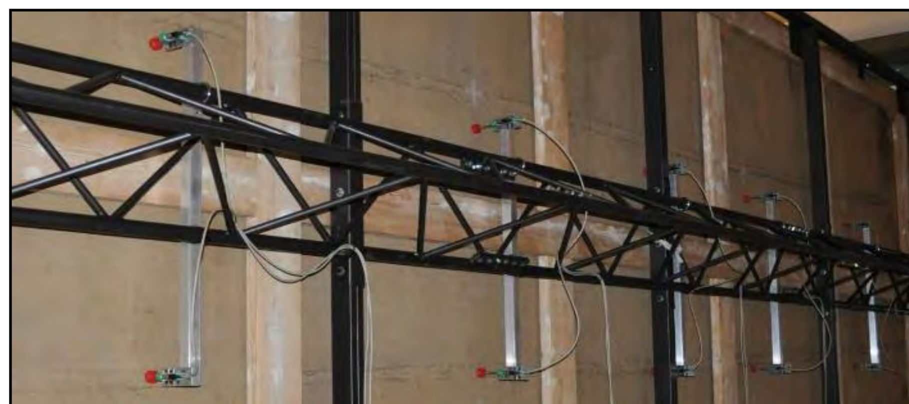

Linear displacement transducers

From: «Tecniche numeriche e sperimentali dell'ingegneria meccanica applicate alla conservazione dei beni culturali». Broggiato, Cortese, Santucci, Torre. Modelli matematici nella conservazione e valorizzazione dei beni culturali. Accademia Nazionale dei Lincei, 15 – 16 dicembre 2015

- Optical experimental setup

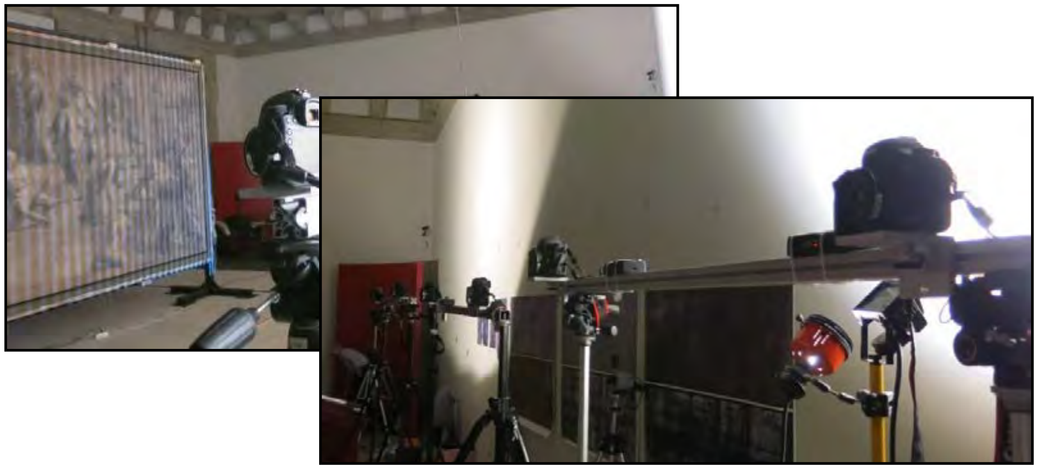

Image acquisition system: 6 Canon EOS 5D-Mark III

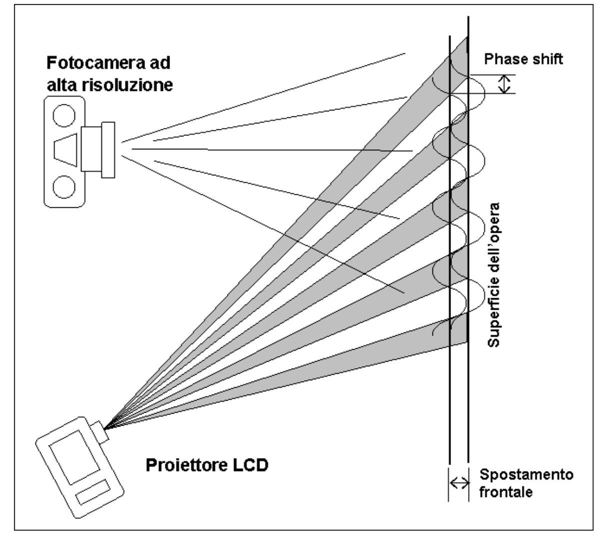

Phase-shift measurement arrangement

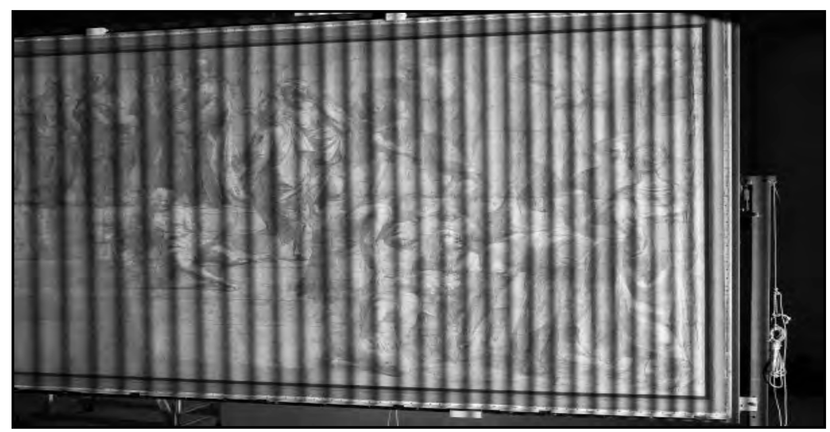

Diffused light and LCD fringe projection systems

❑ Results: compliance of the painting

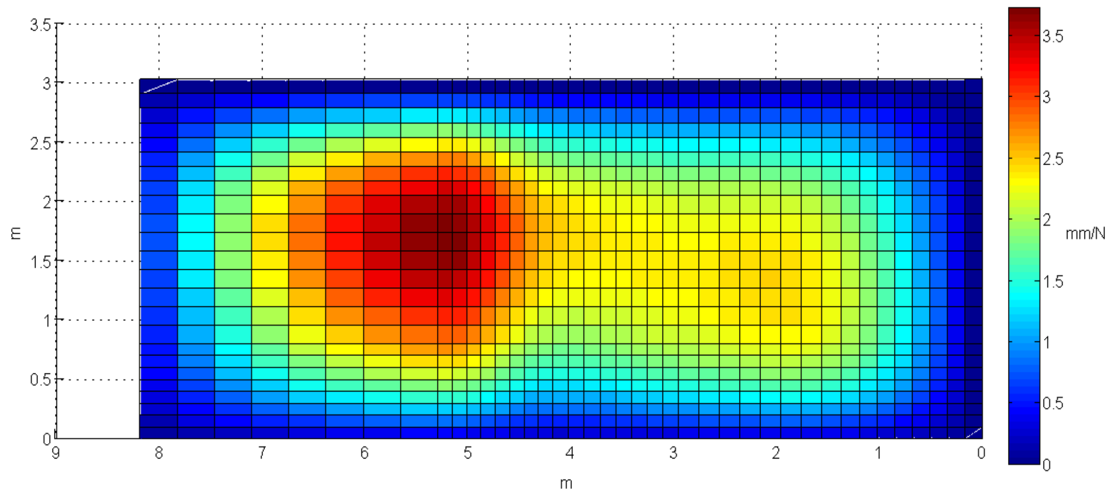

❑ Results: displacement field maps

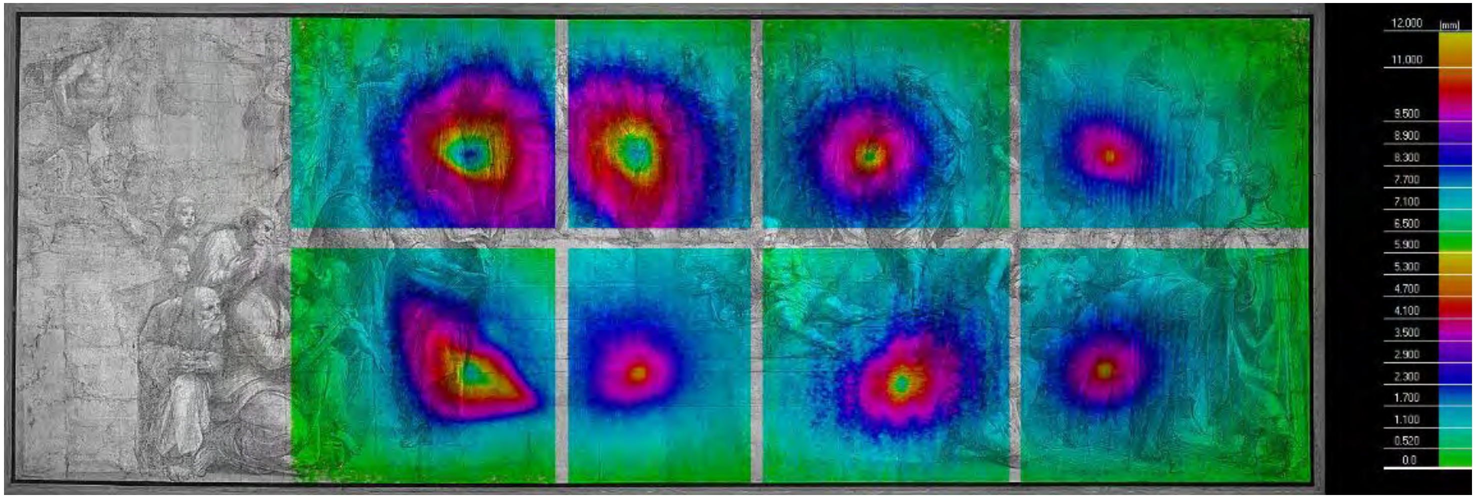

- Results: altimetry of the underformed canvas.

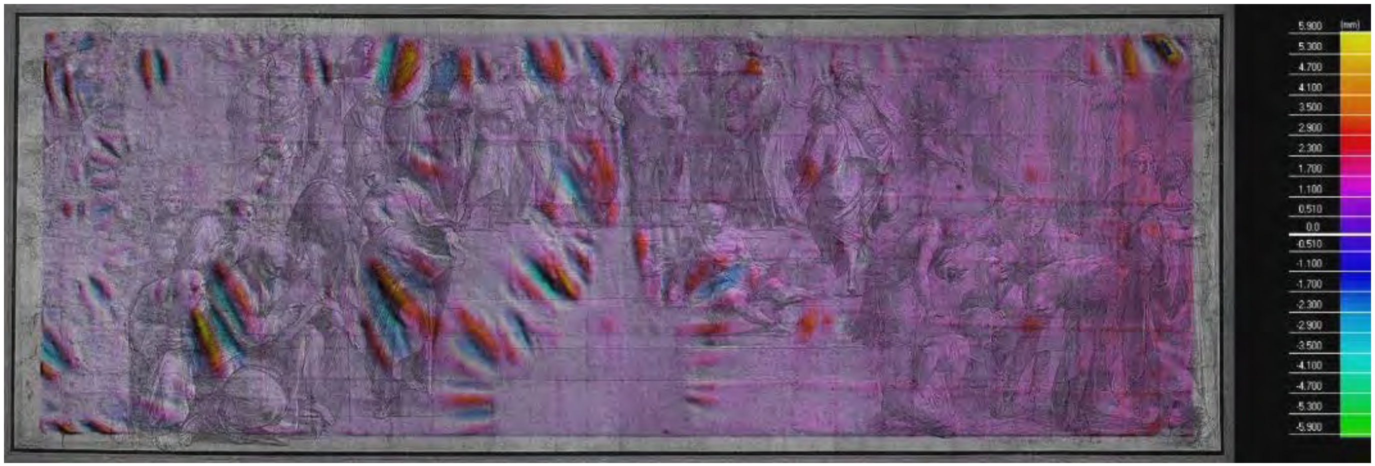

Obtained as the difference between the acquired phase shift map of the actual undeformed canvas and a «virtual» underformed plane

- Defects identification from altimetric data

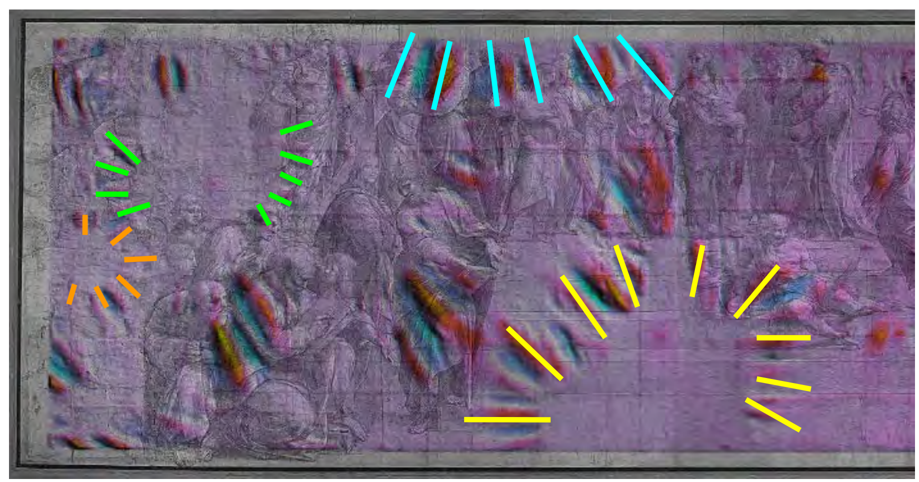

- Artwork: Caravaggio, Resurrezione di Lazzaro,olio su tela, 1609.

380 cm

275 cm

Location: Museo Regionale di Messina.

2012: restoration at Istituto Superiore per la Conservazione ed il Restauro (ISCR) of Rome.

Exhibition: Museo di Roma, 6 giugno – 15 luglio 2012.

- Experiments and Finite Element analysis:

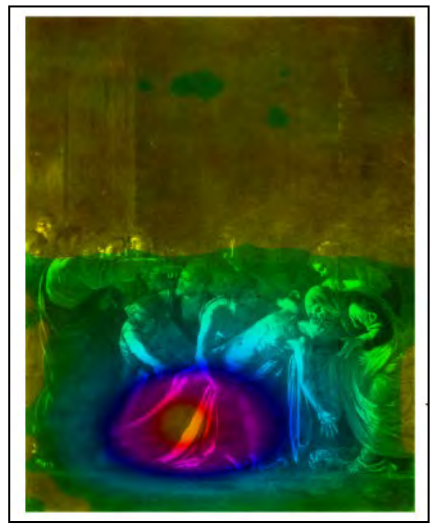

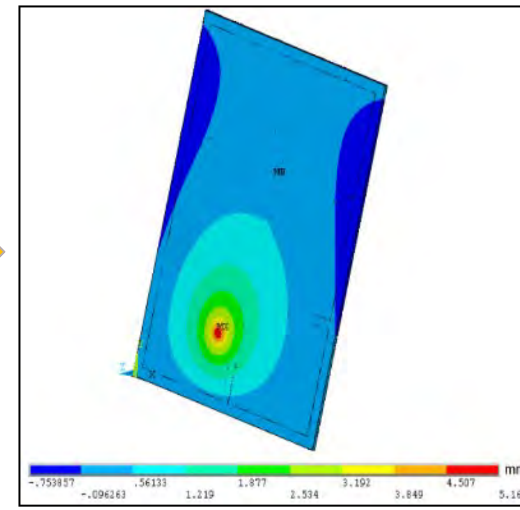

Qualitative estimation of the state of stress in the canvas: identification of average stress by minimization of experimental-numerical out of plane applied displacements

From: «Tecniche numeriche e sperimentali dell'ingegneria meccanica applicate alla conservazione dei beni culturali». **Broggiato, Cortese, Santucci, Torre. Modelli matematici nella conservazione e valorizzazione dei beni culturali.**
Accademia Nazionale dei Lincei, 15 – 16 dicembre 2015

❑ Mechanical characterization of the canvas

Specimen dimensions
260 x 25 x 1.5 mm

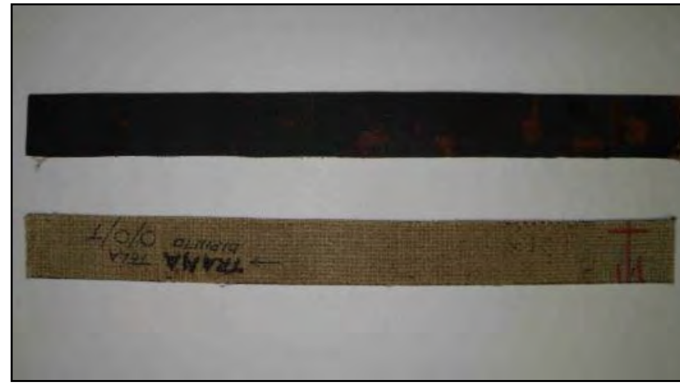

Tensile tests on specimens cut along the two principal orthotropic directions of the canvas

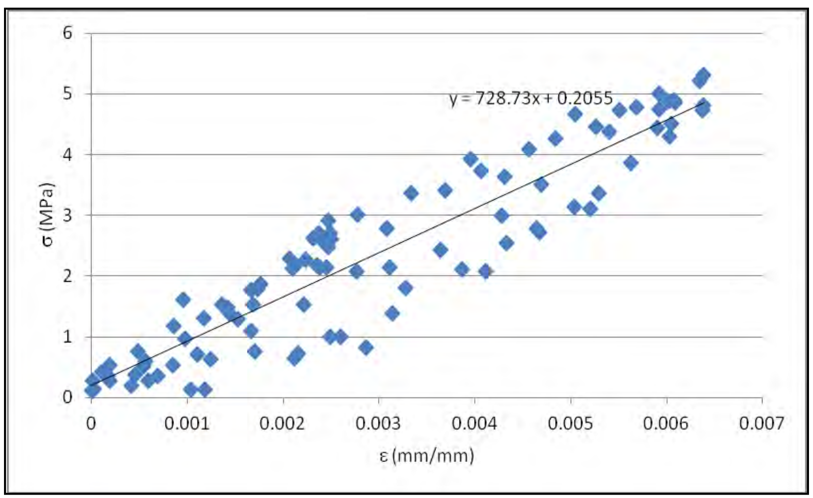

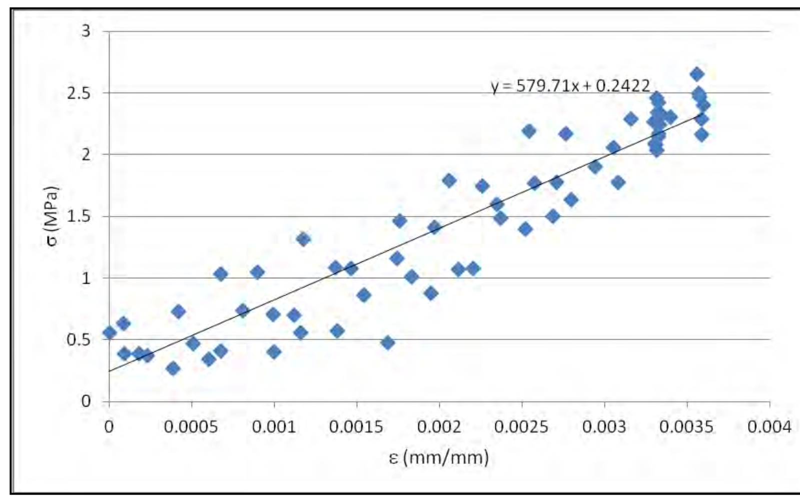

- Finite element model of the artwork, and numerical results.

Out of plane displacement field and von Mises equivalent stress. **Mean initial stress obtained by minimizing the experimental-numerical out of plane displacements.**

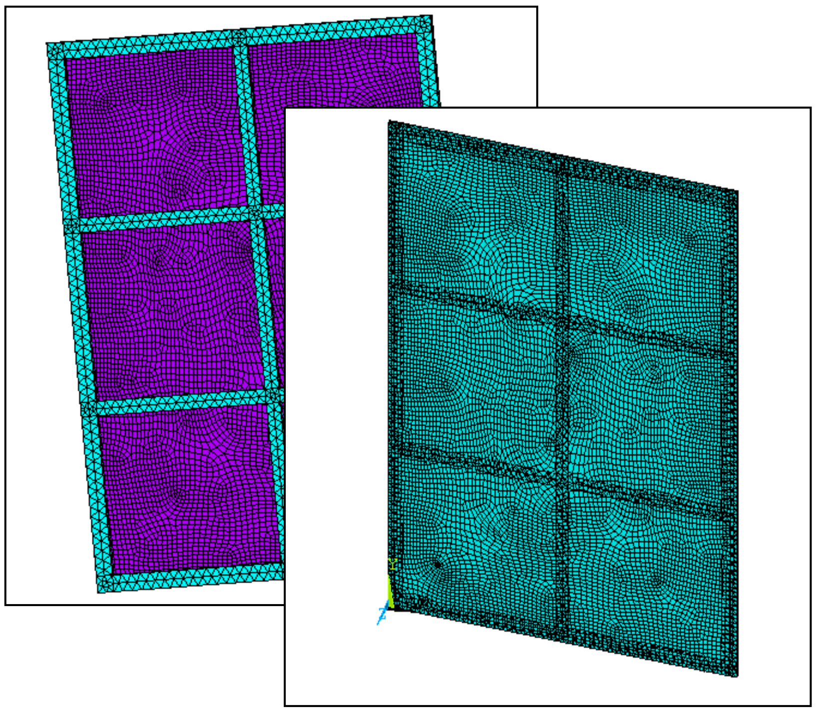

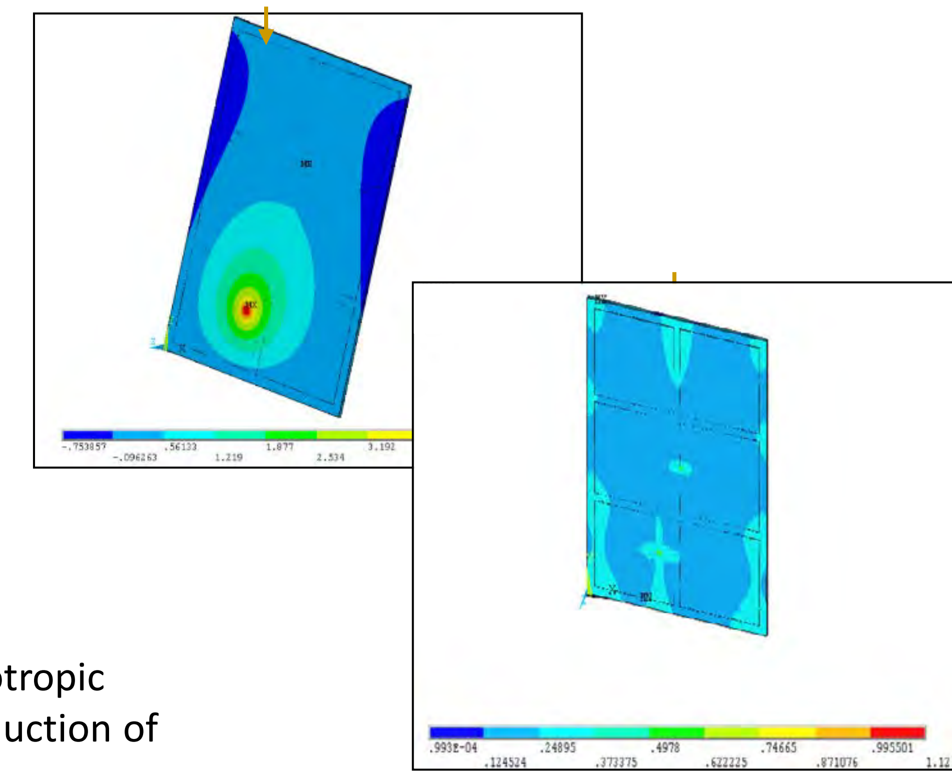

8 node shell and 10 node Tetraedra elements, orthotropic materials behavior, non linear analysis, exact reproduction of experimental boundary and loading condititions

- Numerical results.

Experimental-numerical comparison along significants paths, using best fit mean initial stress in simulation.

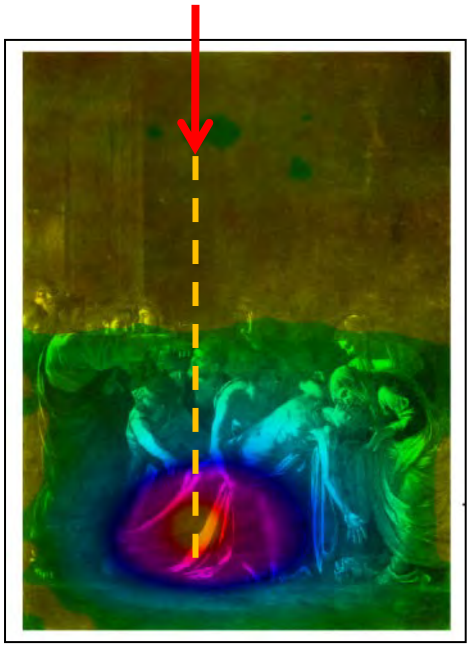

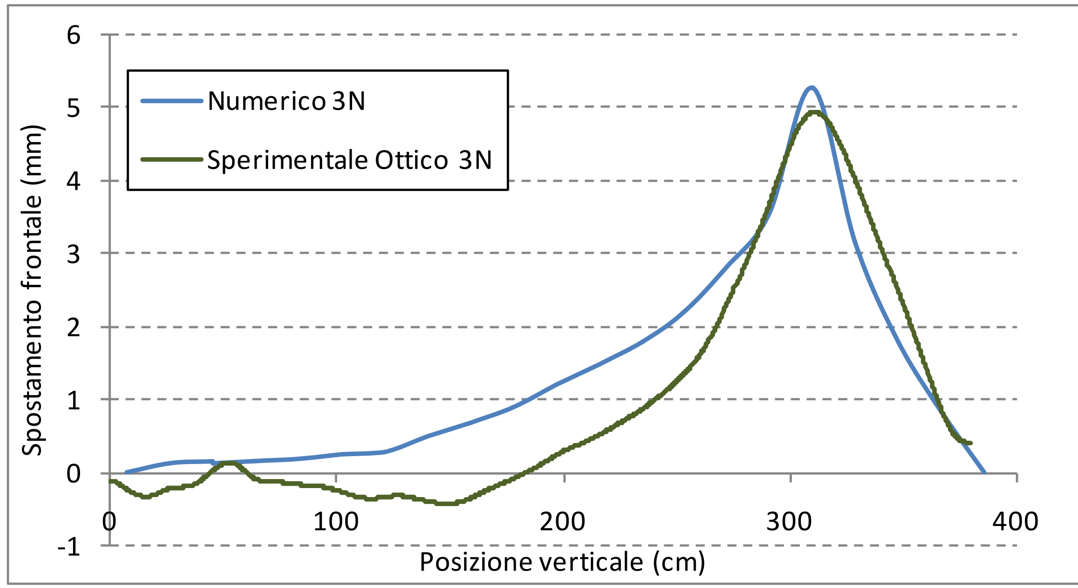

Ongoing research activities

- Anisotropic plasticity models and advanced testing for their calibration and use
- Multiaxial testing and damage models for Additive Manufacturing applications
- Local mechanical characterization of dissimilar welded joints
- Vibro-acoustic analysis of high efficiency epicyclic gears
- Optimum scanning path identification for laser scanning CMM
- Composite structure testing for racing car design
- Innovative drivetrain devising for racing car design
- Remote-Lab project

- Numerical models end experiments for anisotropic materials and parts characterization

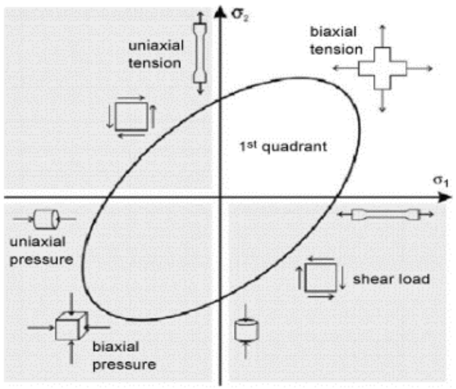

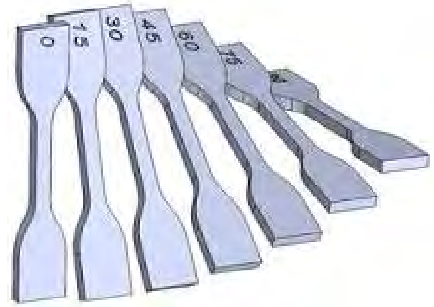

- Many tests are usually required, involving non standard equipment, and consuming time and resources

- Structured light GOM 3D scanner

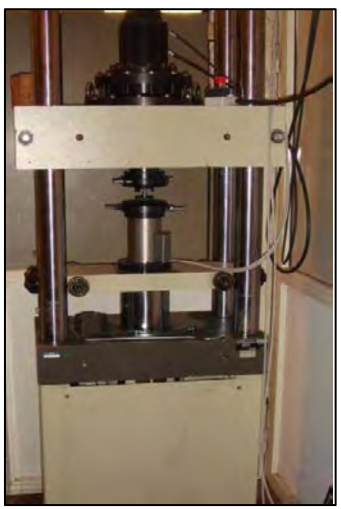

- 3D DIC

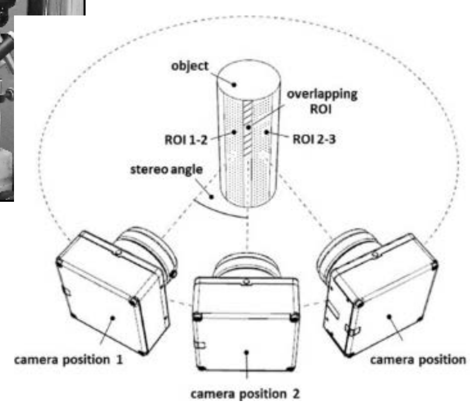

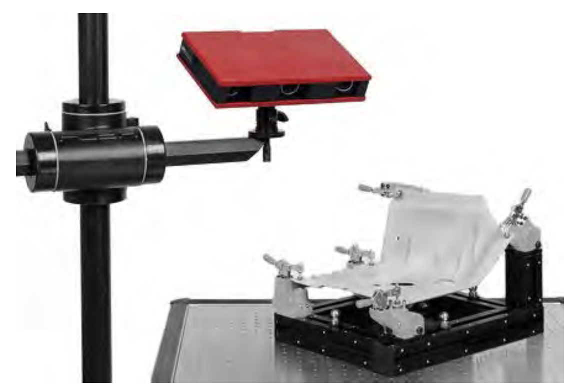

- Use of unconventional smart experimental set-ups to gather local information and quantify material anisotropy

- Calculation of 3d specimen shapes and surface deformation using DIC and 3D Scanner

- Digital images taken at different stages of the test for 3D DIC

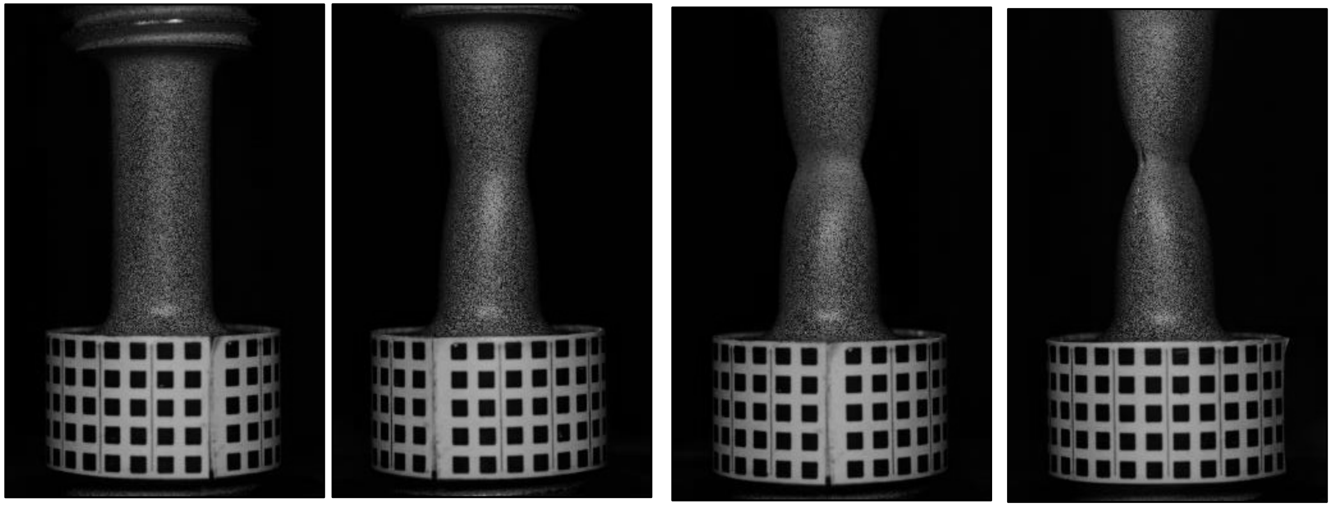

- Point cloud at the same stages from 3D scanner

- Use of unconventional smart experimental set-ups to gather local information and quantify material anisotropy

- In collaboration with UNIBAS and UNIVPM

Ongoing research activities

Multiaxial tests and damage models for Additive Manufacturing

SAPIENZA UNIVERSITÀ DI ROMA

- ❑ Comprehensive multiaxial tests campaign to characterize the structural performance of additive manufacturing materials. Focus on titanium and aluminum alloys.

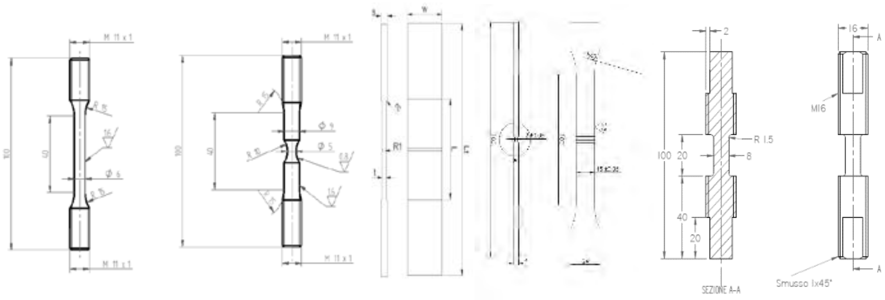

- ❑ Adaptation of damage models to predict failure in additive manufacturing materials and parts.

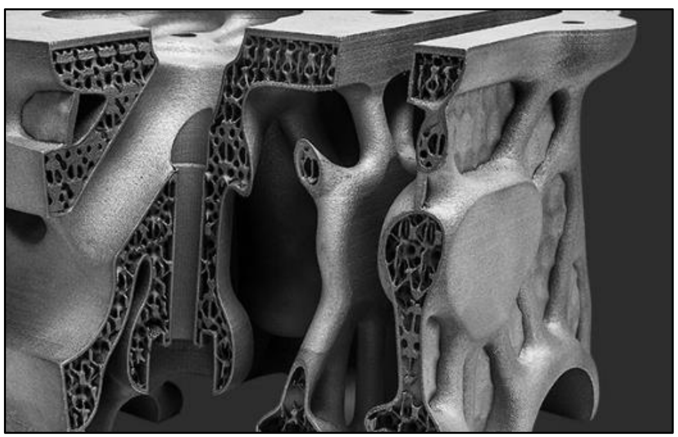

Source: Additive Manufacturing Magazine

Source: Graphite Additive Manufacturing.

- ❑ Validation of model accuracy at laboratory and case study levels

Ongoing research activities

Local mechanical characterization of AHSS dissimilar welded joints

SAPIENZA UNIVERSITÀ DI ROMA

- Testing using “micro”- samples: local assessment of mechanical performance of fusion zone, and heat affected zones in AHSS welded joints for tailored blanks application
- Dissimilar arc welded joint microstructures: focus on arc and laser weldments
- Tensile tests with digital image correlation on micro-specimens, using dedicated grips

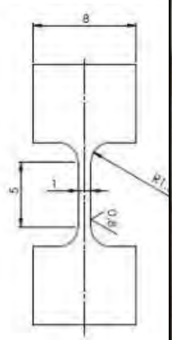

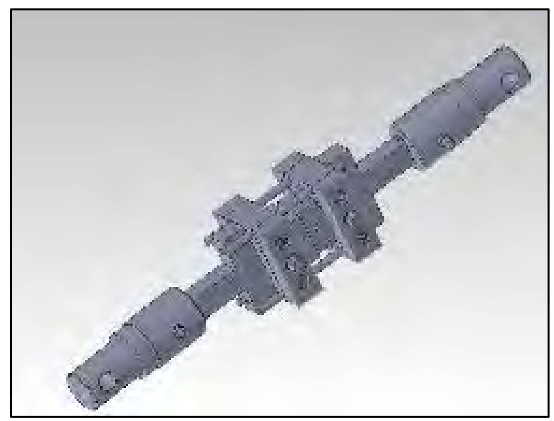

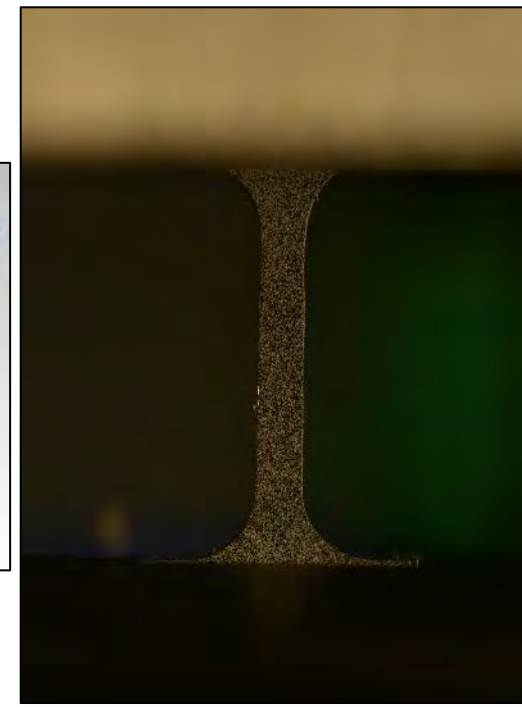

- In collaboration with the Faculty of Science and Technology of UNIBZ

- Nikon scanning head

- Scanning path identification

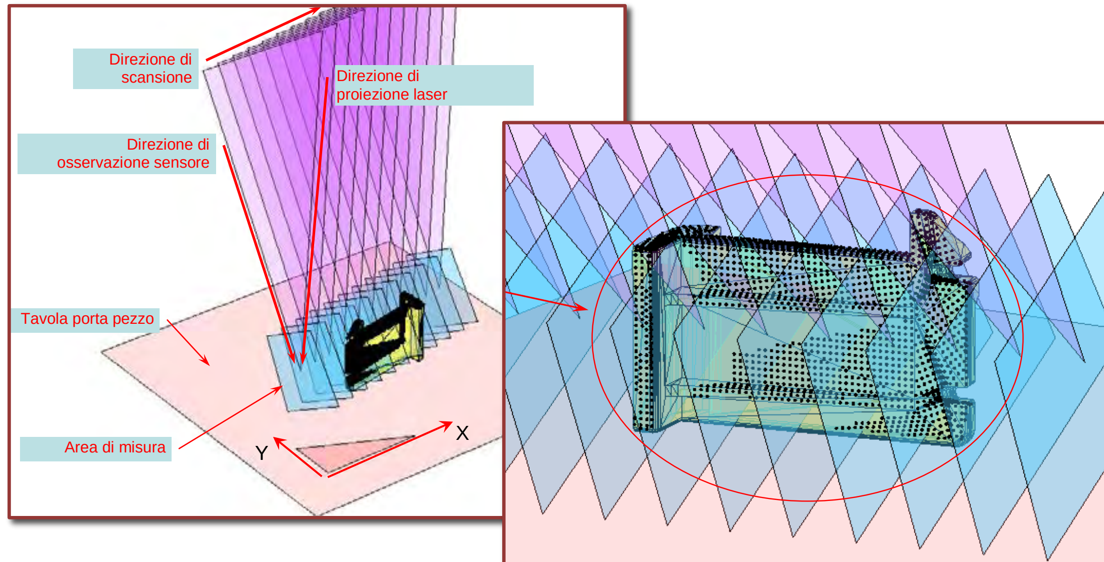

- Simulated acquired point cloud (occlusion test)

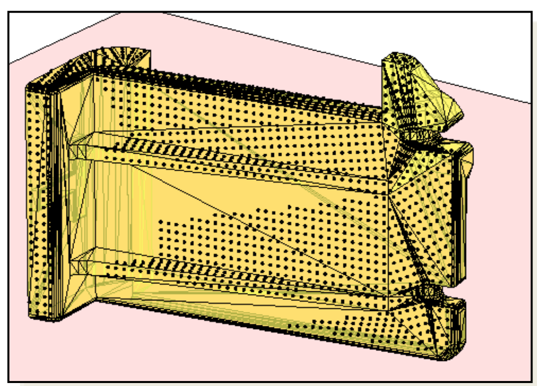

- Optimum scanning paths

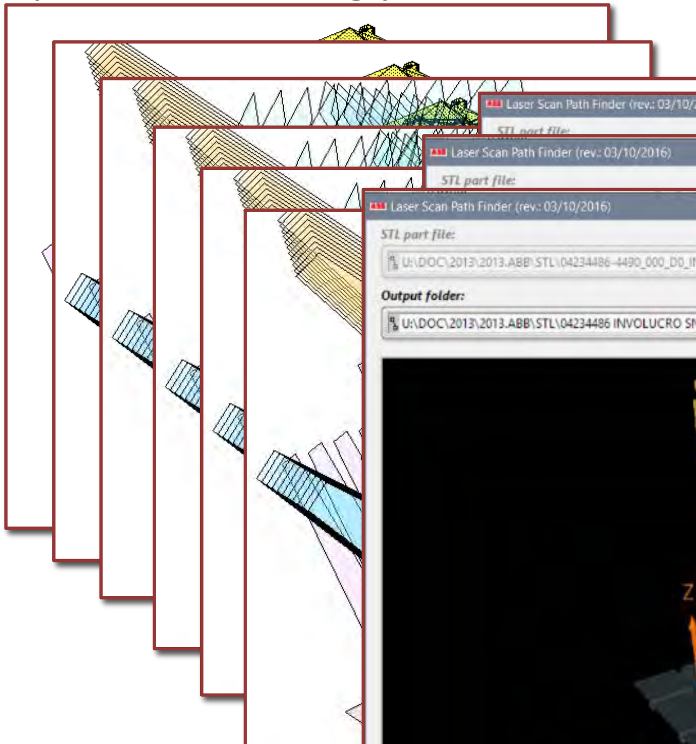

- Graphical user interface

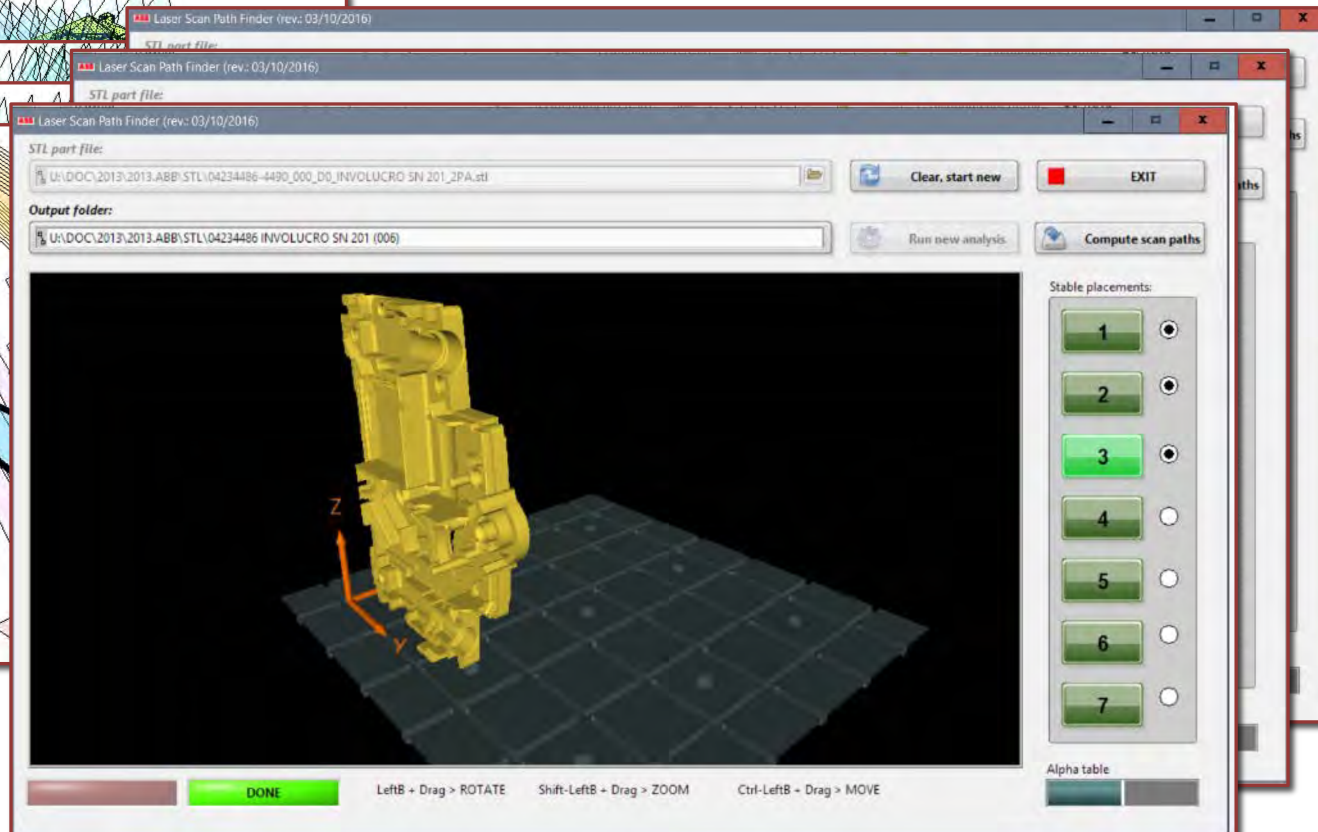

- Static Three Point Bending test

- Shea

- Harness attachment test

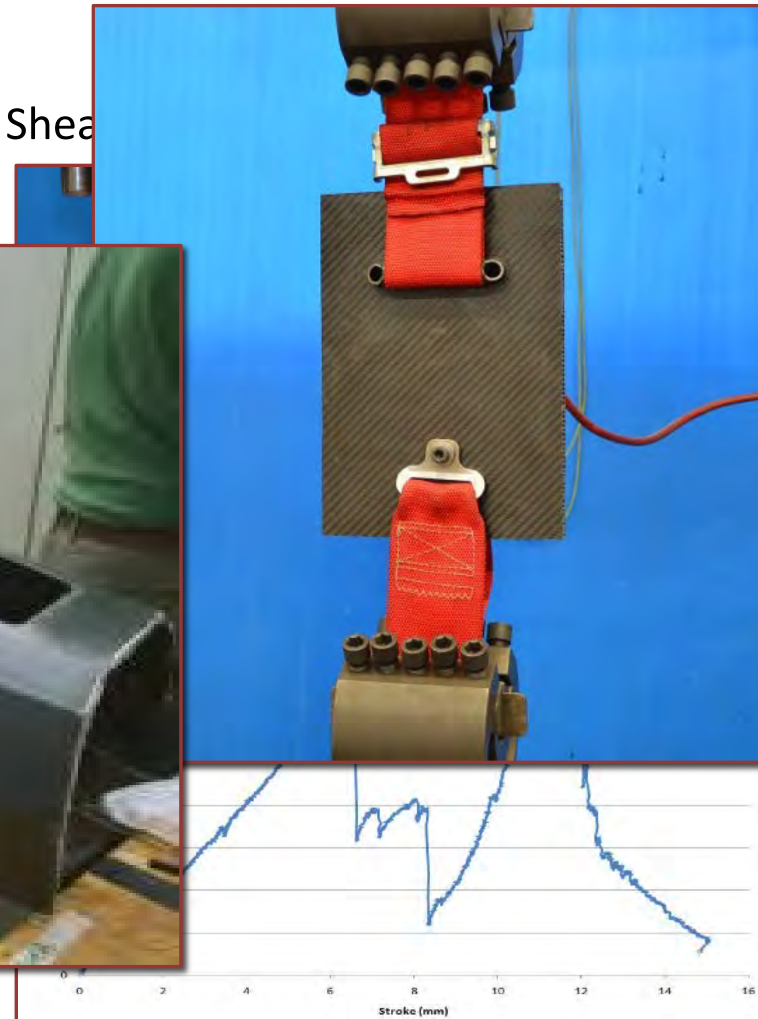

Ongoing research activities

Composite structure testing for racing car design

- Impact attenuator crash test

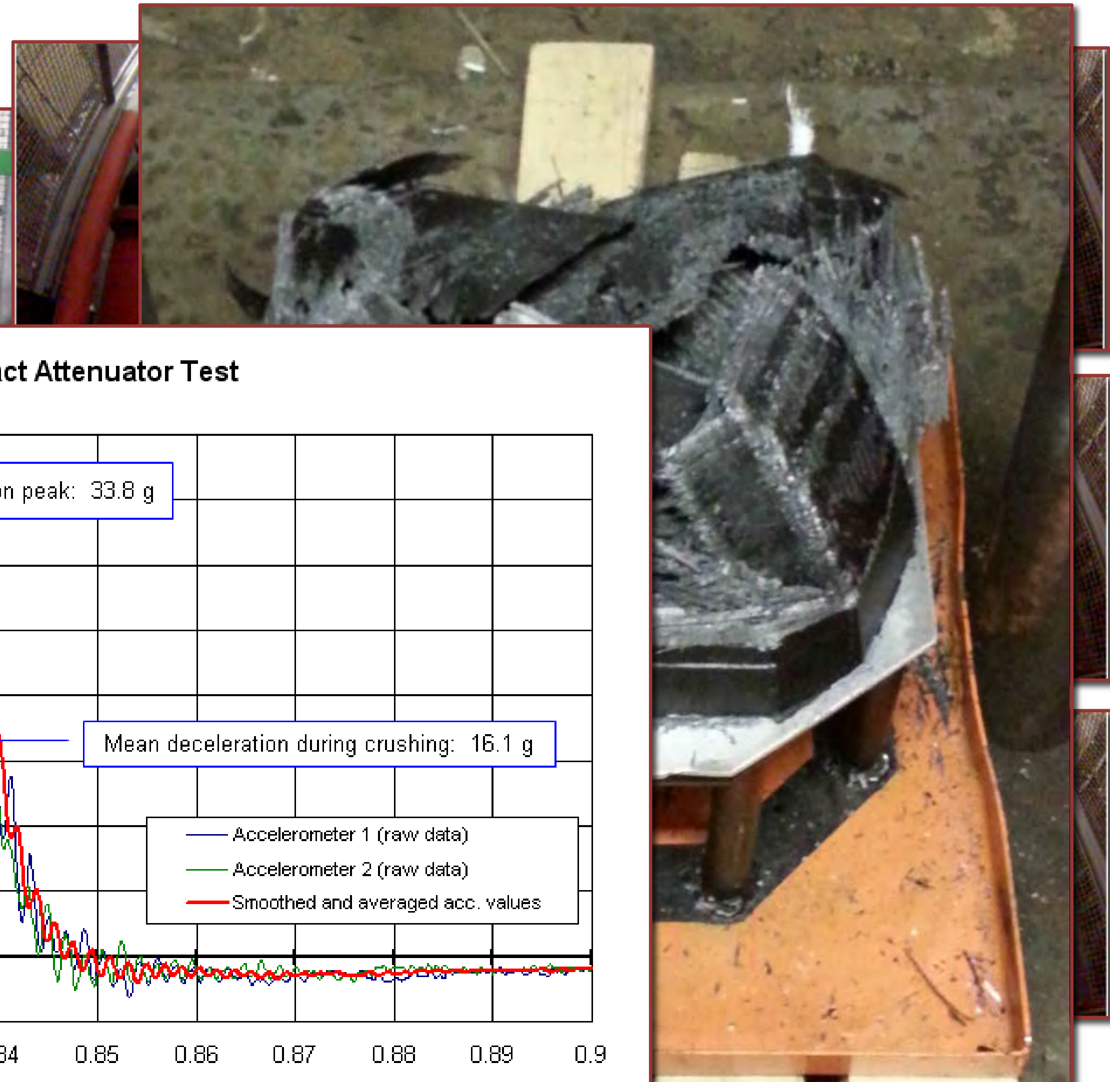

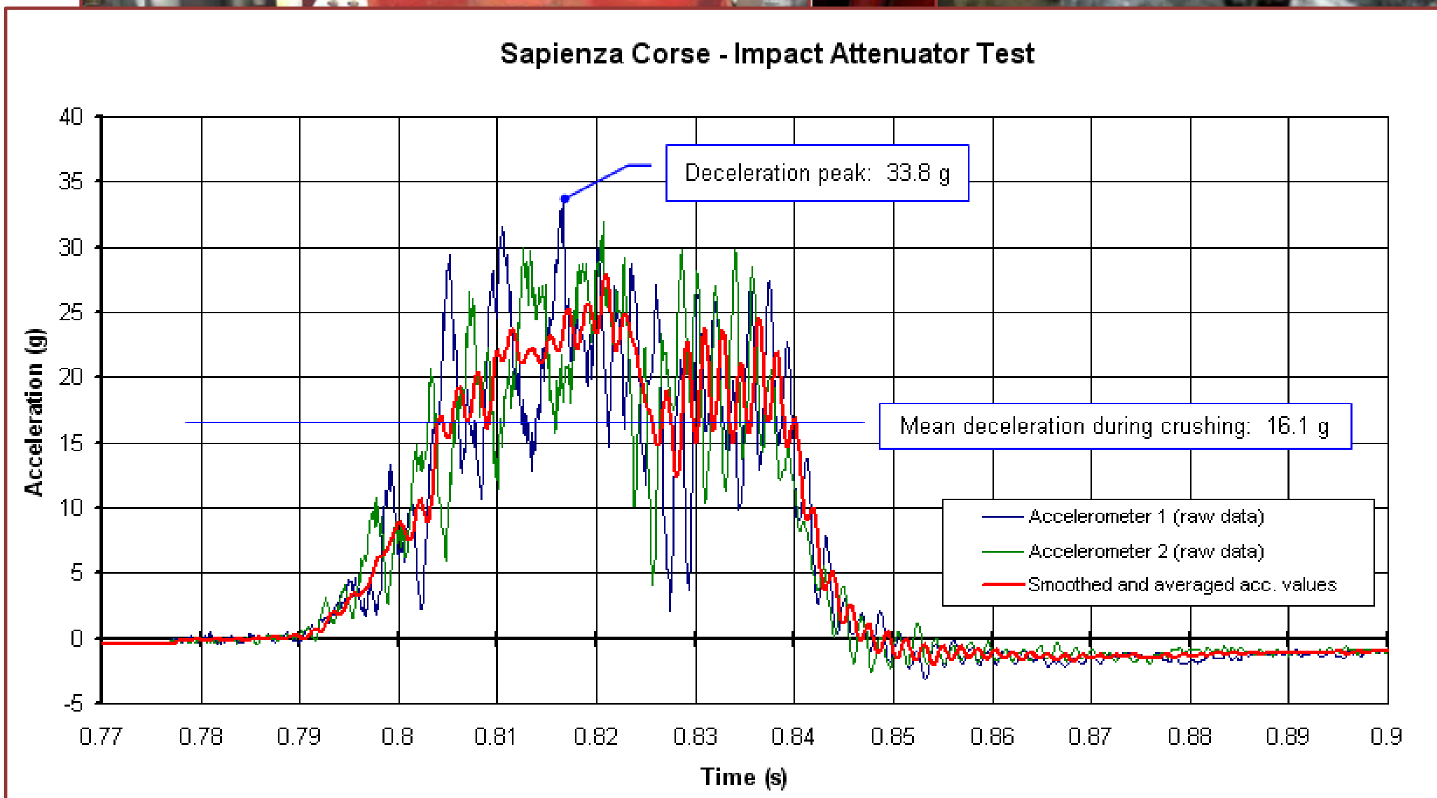

- ❑ Four Wheel Drive & Electronic Controlled Torque Vectoring drivetrain

- ❑ Conventional 4WD drivetrain

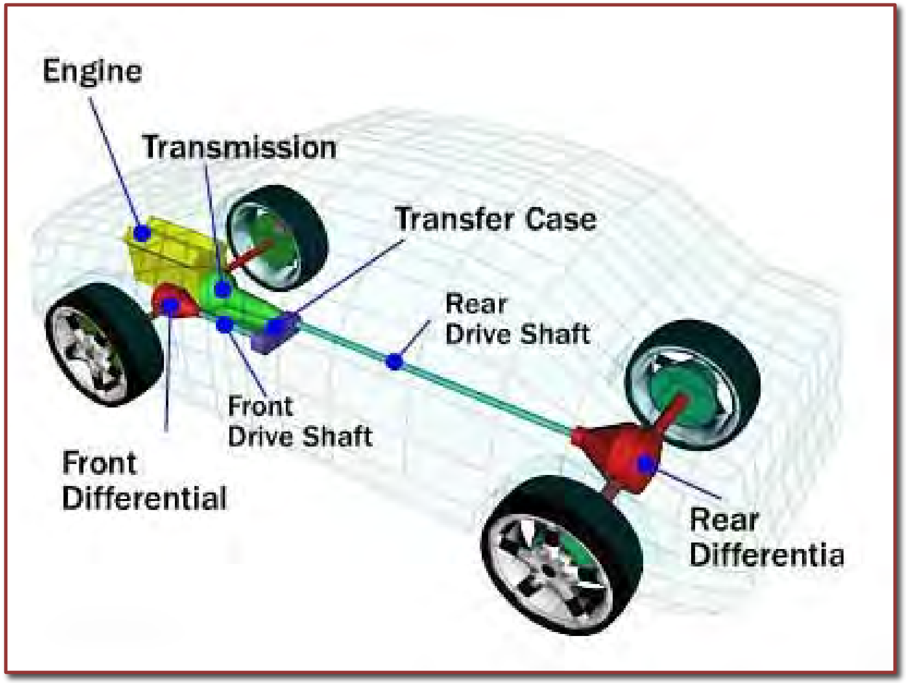

Ongoing research activities

Innovative drivetrain devising for racing car design

- Electronic Controlled Torque Vectoring

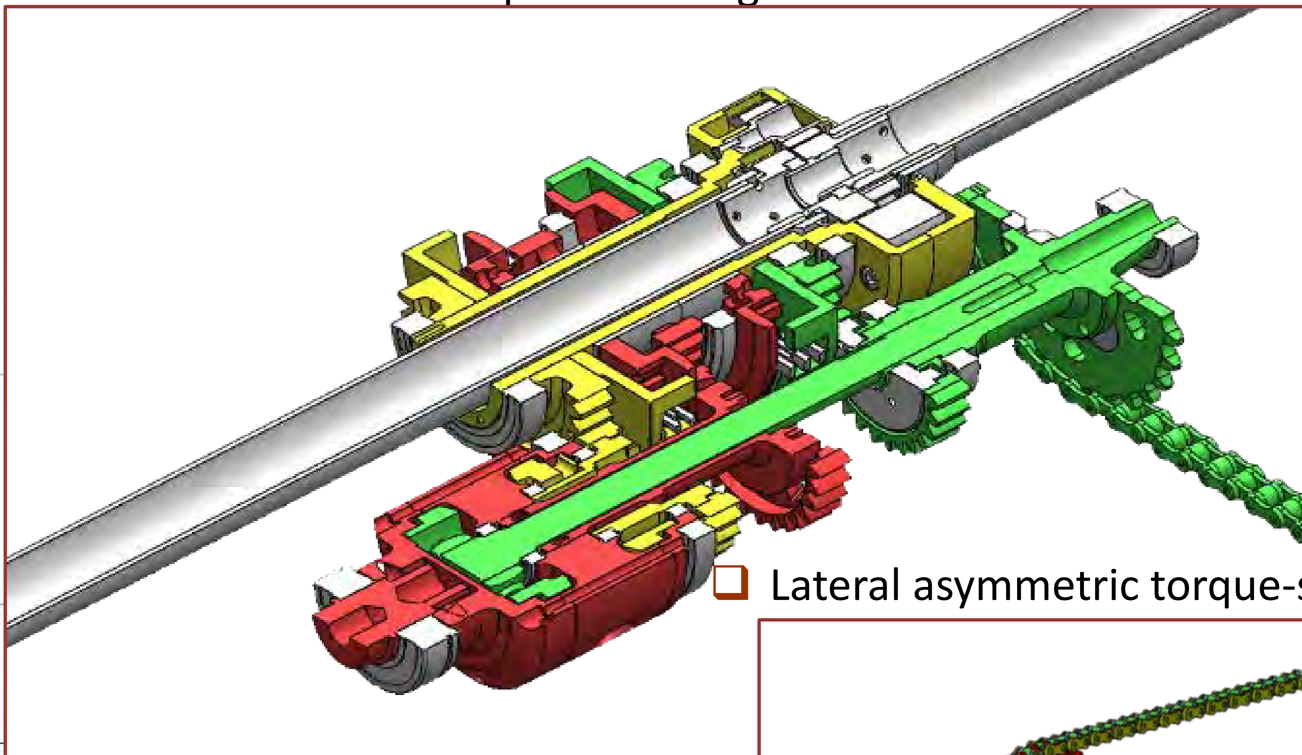

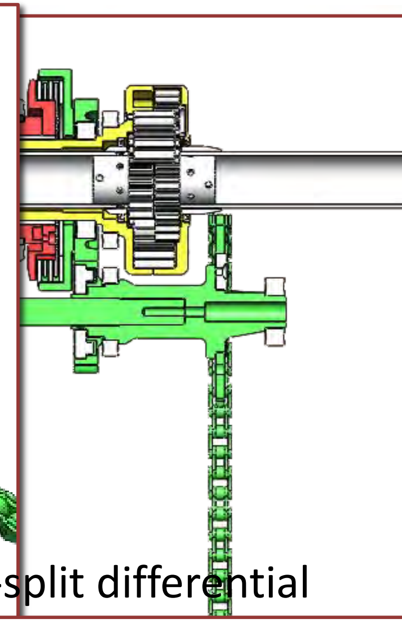

- Lateral asymmetric torque-split differential

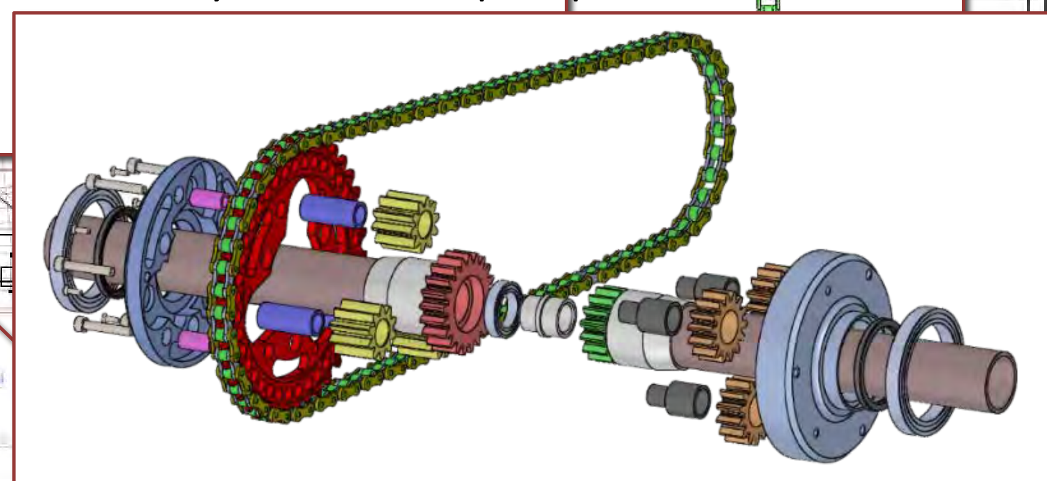

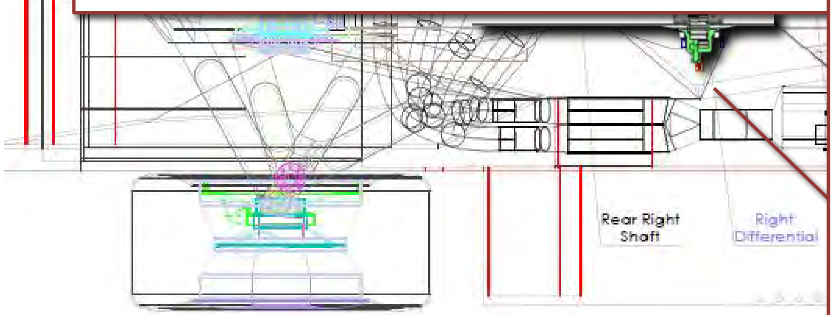

Ongoing research activities

Remote-Lab project

- ❑ Wheel-to-road rolling contact test bench
- ❑ MTS tire test bench

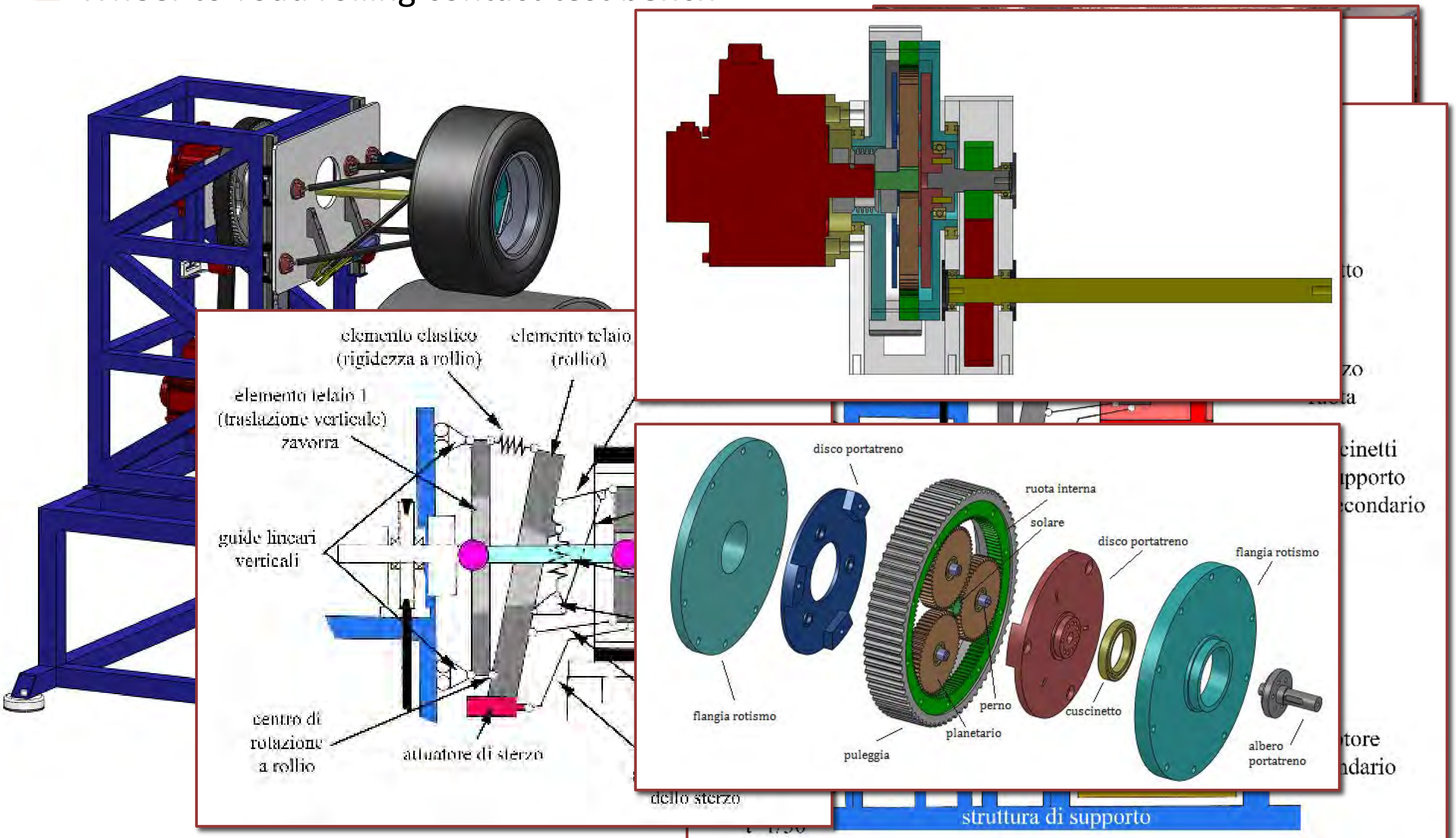

Thank you for your attention